

University of Montana

## ScholarWorks at University of Montana

---

Graduate Student Theses, Dissertations, &  
Professional Papers

Graduate School

---

1996

### Anomalous platinum-group element occurrence below the JM Reef Stillwater Complex Montana

C. L. McIlveen  
*The University of Montana*

Follow this and additional works at: <https://scholarworks.umt.edu/etd>

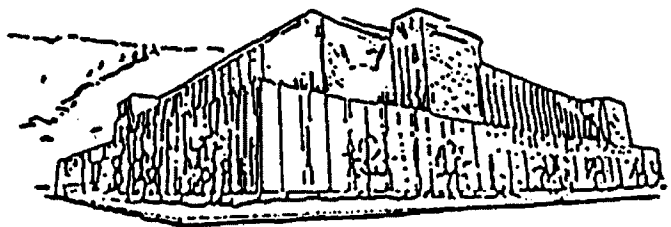
**Let us know how access to this document benefits you.**

---

#### Recommended Citation

McIlveen, C. L., "Anomalous platinum-group element occurrence below the JM Reef Stillwater Complex Montana" (1996). *Graduate Student Theses, Dissertations, & Professional Papers*. 7580.  
<https://scholarworks.umt.edu/etd/7580>

This Thesis is brought to you for free and open access by the Graduate School at ScholarWorks at University of Montana. It has been accepted for inclusion in Graduate Student Theses, Dissertations, & Professional Papers by an authorized administrator of ScholarWorks at University of Montana. For more information, please contact [scholarworks@mso.umt.edu](mailto:scholarworks@mso.umt.edu).



Maureen and Mike  
**MANSFIELD LIBRARY**

The University of **MONTANA**

---

Permission is granted by the author to reproduce this material in its entirety,  
provided that this material is used for scholarly purposes and is properly cited in  
published works and reports.

**\*\* Please check "Yes" or "No" and provide signature \*\***

Yes, I grant permission

No, I do not grant permission

Author's Signature

Date

12-20-96

Any copying for commercial purposes or financial gain may be undertaken only with  
the author's explicit consent.



**AN ANOMALOUS PLATINUM-GROUP ELEMENT  
OCCURRENCE BELOW THE JM REEF, STILLWATER  
COMPLEX, MONTANA**

by

**C. L. McIlveen**

**B. S., The University of the South, 1990**

**submitted in partial fulfillment of the requirements**

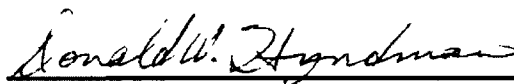
**for the degree of**

**Master of Science**

**The University of Montana**

**1996**

**Approved by:**



**Chairperson**



**Dean, Graduate School**



**Date**

UMI Number: EP38381

All rights reserved

**INFORMATION TO ALL USERS**

The quality of this reproduction is dependent upon the quality of the copy submitted.

In the unlikely event that the author did not send a complete manuscript and there are missing pages, these will be noted. Also, if material had to be removed, a note will indicate the deletion.



UMI EP38381

Published by ProQuest LLC (2013). Copyright in the Dissertation held by the Author.

Microform Edition © ProQuest LLC.

All rights reserved. This work is protected against  
unauthorized copying under Title 17, United States Code



ProQuest LLC.  
789 East Eisenhower Parkway  
P.O. Box 1346  
Ann Arbor, MI 48106 - 1346

**An Anomalous Platinum-Group Element Occurrence Below The JM Reef, Stillwater Complex, Montana**Director: Donald H. Hyndman *DWH*

The Coors 602 zone is an anomalous, laterally discontinuous zone containing significant platinum group element (PGE) mineralization. The area lies below the JM reef platinum horizon. The Coors area is associated with the first occurrence of cumulus plagioclase, but most of the significant anomalous PGE values occur in discordant, pegmatoidal bronzitites which are within the Norite I zone. PGE mineralization predominantly occurs in bronzitite patches within noritic rocks, rather than olivine-bearing rocks as it does in the JM Reef. The Coors bronzitites are texturally and chemically distinct from bronzitites in the Ultramafic zone below. Most of the Coors bronzitites are pegmatoidal with only about 1-2 percent interstitial plagioclase. Magnesium numbers in the bronzitites decrease up-section along trend from the Bronzitite zone, however, the mineralized samples show significantly lower numbers. Nor do these mineralized samples appear to be directly related to the reef rocks either. Rock types as well as the palladium : platinum ratio differ between the Coors 602 zone and the JM Reef package. Pd/Pt in the JM reef averages about 3:1, whereas the Coors zone contains ratios closer to 1:1.

The mineralized bronzitites in the Coors 602 zone are spatially associated with many anomalous features, including disturbed layering, discordant units, and the thinning or absence of a stratigraphic unit. These features are common throughout the Complex, but not at such large scales (hundreds of feet versus inches). The irregularities in stratigraphy appear to be the result of physical disturbances related to magmatic currents associated with an influx of a new magma. This new influx of magma may also have caused the precipitation of PGE sulfides. Volatiles likely caused the formation of the pegmatoids. The entire Coors zone likely represents a pothole similar to those found in the Bushveld Complex. Because of the PGE association, it is important to know if these irregular features in the Coors zone are genetically related to the mineralization. Determining this relationship, the origin of mineralization and the significance of the stratigraphic location of this zone are important, as this anomalous zone may represent a potential target for exploration elsewhere in the Stillwater and in other layered mafic intrusions.

## **ACKNOWLEDGEMENTS**

**My thanks and gratitude go out to Don Hyndman for all of his guidance, support, and especially his continued motivation throughout the years. I would also like to thank Steve Sheriff and Richard Field for serving on my committee. I would like to thank the U.S. Geological Survey and Amoco Production Company, in particular Sara Foland for their financial support for this work. I would especially like to thank Michael Zientek (USGS) for sharing his insight into the Stillwater Complex with me. Without Michael, this thesis would not have been possible. I would also like to thank the Stillwater Mining Company for their assistance in all aspects of my field work. Field assistants whom I would like to thank include Pete Ellsworth, Josh Gladden, Abbey Walden, and Langdon Mitchell. Others who supported me during this whole process that I would like to thank are Steen Simonsen, Robin Shropshire, an especially my husband John Walden.**

# TABLE OF CONTENTS

ABSTRACT .....	ii
ACKNOWLEDGEMENTS .....	iii
TABLE OF CONTENTS .....	iv
LIST OF TABLES .....	v
LIST OF FIGURES .....	vi
I. INTRODUCTION .....	1
GENERAL GEOLOGY .....	2
PROBLEMS AND OBJECTIVES .....	9
II. COORS-602 AREA .....	12
LOCATION AND GENERAL GEOLOGY .....	12
METHODS .....	15
FIELD RELATIONSHIPS .....	19
Bronzitite in Norite I .....	19
Disturbed Stratigraphy .....	21
Pegmatoids .....	26
PGE Mineralization .....	27
MINERALOGY AND PETROLOGY .....	28
Bronzitite .....	28
Norite .....	30
Sulfides .....	30
Alteration .....	31
Resorption .....	31
GEOCHEMISTRY .....	34
Silicate .....	34
PGE Sulfides .....	43
III. INTERPRETATIONS .....	49
JM REEF .....	49
PHYSICAL DISTURBANCE .....	53
Strong Currents, Turbulent Mixing of Magma, and Magmatic Erosion .....	53
Topography in the Magma Chamber .....	55
Slumping, Compaction, and Faulting During Formation .....	59
CHEMICAL DISTURBANCES .....	61
Mg Number .....	61
Resorption .....	63
Increase in $f_{H_2O}$ .....	63
PGE Mineralization Below the JM Reef .....	65
IV. SUMMARY AND CONCLUSION .....	
V. REFERENCES CITED .....	69
VI. APPENDICES .....	70
Appendix A: Johns-Manville Company Outcrop Map .....	pocket
Appendix B: USGS Geochemical Analyses (disk) .....	pocket



## LIST OF TABLES

<u>Table</u>	<u>Page</u>
1. Terminology for describing rocks of the Stillwater Complex .....	6
2. USGS geochemical analytical methods .....	18
3. Sample description including rock type, grain size, percent orthopyroxene and approximate percent sulfide .....	29
4. Electron microprobe analyses of orthopyroxene from the Coors area and Mouat Mine road given in weight percent .....	35
5. Microprobe data for figure 10 including Mg number, height, and rock type ..	38
6. Whole rock analyses (XRF) of Coors area and Mouat Mine road .....	39,40
7. Data for figure 11 including Mg number, height, and rock type .....	42
8. Assay data including PGE analyses from four exploration trenches in the Coors area .....	44
9. PGE, Cu and Ni Data for Coors area and Mouat Mine road samples .....	45

## LIST OF FIGURES

<u>Figure</u>	<u>Page</u>
1. Geologic map of the Beartooth Mountains .....	3
2. Stratigraphic subdivisions of the Stillwater Complex .....	5
3. Schematic columnar section for the Stillwater Complex showing relative locations of sulfide, platinum-group-element and chromite mineralization, and representative analyses of rocks .....	10
4. Simplified geologic map of the Stillwater Complex showing location of Coors anomaly .....	13
5. Outcrop map (1"=400') prepared by geologists at Johns-Manville Company .....	14
5a. Outcrop map (1"=100') prepared by geologists at Johns-Manville Company .....	pocket
6. Sample location map (1"= 400') from the Coors area. Note: use in combination with figure 5.....	16
7. Sample outcrop sketches showing irregular layering and truncating features...	24
8. Simplified map of the Stillwater Complex showing location of Janet 50 .....	25
with respect to Coors.	
9. Pressure - temperature diagrams for a dry magma and a water undersaturated magma and temperature-composition diagrams for a binary system .....	32
10. Plot of stratigraphic height versus Mg number based for microprobe data of orthopyroxene .....	37
11. Plot of stratigraphic height versus Mg number of whole rocks .....	41
12a. Plot of Pd versus Pt for trench samples in the Coors area .....	46
12b. Plot of Pd versus Pt for Coors area and Mouat mine road samples .....	46
13a. Plot of Cu and Ni versus Pd for trench samples in the Coors area .....	47
13b. Plot of Cu and Ni versus Pd for Coors area and Mouat mine road samples ...	47

14a. Plot of Cu and Ni versus Pt for trench samples in the Coors area .....	48
14b. Plot of Cu and Ni versus Pt for Coors area and Mouat mine road samples..	48
15. Schematic diagram illustrating the variation in the solubility of iron sulfide with fractionation .....	50
16. The effect of variations in the silicate:sulfide ratio ( $R$ ) on the precious metal content of a sulfide liquid for different values of $D$ .....	51
17. Schematic model of disturbed layering in the Coors area .....	56
18.. Reconstruction of the base of the Stillwater Complex showing idealized basins and topographic highs at the time of JM Reef deposition .....	57
19. Conceptual view of basin and ridge development before Laramide deformation in the eastern part of the Stillwater Complex .....	58
20. Schematic diagram showing disturbed layering caused by a crystallized block slumping off a topographic high .....	60

## **INTRODUCTION**

Mafic to ultramafic layered intrusions are unique not only because they host the majority of the world's platinum-group element and chromium deposits, but because they also provide an excellent opportunity to study magmatic processes in a natural system. Concentrations of platinum-group elements (PGE's) in most of these intrusions occur as laterally continuous horizons referred to as reefs. An exception to this occurs in the Stillwater Complex. In addition to the reef, there is an anomalous, laterally discontinuous area known as the Coors 602 zone contains significant PGE mineralization. The area is associated with the first occurrence of cumulus plagioclase, but most of the significant anomalous PGE values occur in discordant, pegmatoidal bronzitites which are within the Norite I Zone.

The Coors 602 zone is studied in detail in this paper to determine the origin of mineralization and the significance of the stratigraphic location as another possible ore target in these intrusions. Coors mineralization predominantly occurs in bronzitite patches within noritic rocks, rather than olivine-bearing rocks as it does in the JM Reef. The Coors bronzitites are texturally and chemically distinct from bronzitites in the Ultramafic Zone below. They do not appear to be related to the reef rocks either. Rock types as well as the Pd/Pt ratio differ between the Coors 602 zone and the JM Reef package.

The mineralized bronzitites in the Coors 602 zone are spatially associated with many anomalous features, including disturbed layering, discordant units, and the thinning or absence of a stratigraphic unit. The irregularities in stratigraphy appear to be the result of physical disturbances related to magmatic currents associated with an influx of a new

magma. Because of the PGE association, it is important to know if these irregular features are genetically related to the mineralization.

## **GENERAL GEOLOGY**

The Stillwater Complex, a late Archean, 2.70 b.y., mafic to ultramafic layered intrusion, lies in south-central Montana, along the northeast front of the Beartooth Mountains (Fig. 1). The complex crops out for about 48 kilometers along an approximate N 70° W strike; it has an exposed thickness of 5.5 kilometers and a width of 7 kilometers (Page and Zientek, 1985; Zientek et al., 1985; Jackson, 1961). Kleinkopf (1985) suggests, through gravity studies, that the intrusion may extend 25 kilometers to the northeast under Phanerozoic rocks. Xenoliths of the Stillwater Complex in Tertiary-Cretaceous intrusions north of the exposed portion of the complex support Kleinkopf's interpretation (Brozdowski, 1985).

The complex was emplaced into Middle Archean metasedimentary rocks, now exposed below the southern contact of the Stillwater Complex. The upper part of the intrusion, to the northeast, was removed by erosion and is unconformably overlain by Paleozoic and Mesozoic sedimentary rocks. Structural deformation occurred prior to middle Cambrian time and again during the Laramide orogeny; the complex now dips steeply to the north and is locally overturned (Page and Zientek, 1985). Jones et al. (1960), Page and Nokleberg (1974), Segerstrom and Carlson (1982), and others have

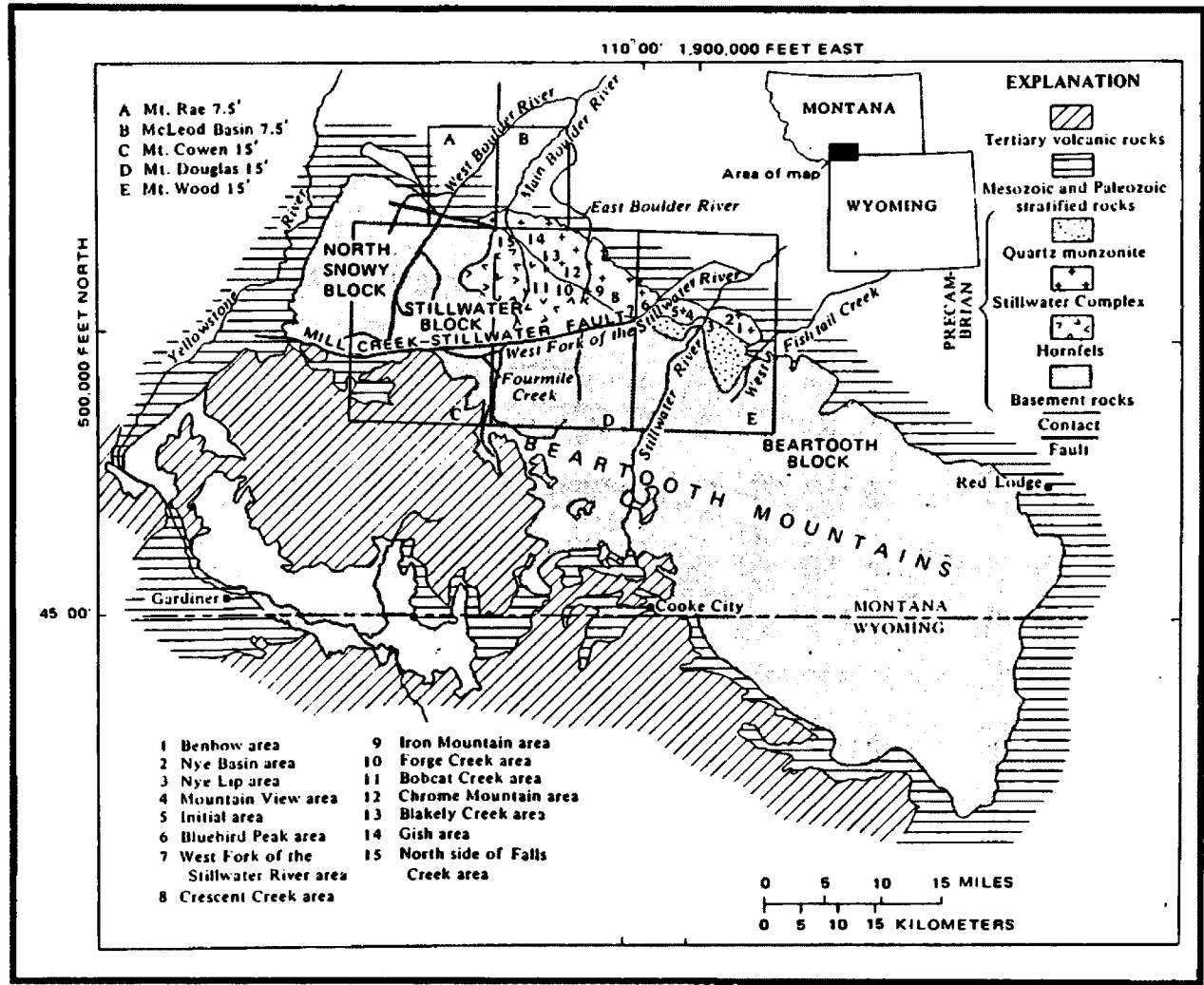


Figure 1. Simplified geologic map of the Beartooth Mountains showing location of the Stillwater Complex (modified from Page and Zientek, 1985).

published detailed descriptions of the structure and geologic setting of the Stillwater Complex.

McCallum et al. (1980), described the stratigraphic units of the Stillwater Complex used in this paper (Fig. 2). They subdivided the layered cumulates into five major stratigraphic units: the Basal Series, the Ultramafic Series, and the Lower, Middle, and Upper Banded Series. The cumulate terminology used in this paper are listed in Table 1. Original views on the genesis of layered intrusions evoked gravity settling as the primary means of producing layered cumulates (Hess, 1960; Jackson, 1961; and others). More recent work has strongly suggested other mechanisms to be more important than crystal settling in the formation of these intrusions (Campbell, 1978; Irvine, 1980). Irvine et al, 1983, suggest "cumulus" layering resulted from in situ crystallization and downdip accretion in a stratified liquid. Although the definition of cumulates involves processes, the term cumulus in this paper, and other recent papers (Campbell, 1978; Todd et al., 1982), is used descriptively with no genetic implications.

The Basal Series consists primarily of bronzite-rich cumulates. The base of this unit forms the intrusive contact with the metasedimentary rocks beneath the complex. Thickness is variable and the unit is missing in some places (Zientek et al., 1985). The contact between the Basal Series and the overlying Ultramafic Series is marked by the appearance of significant amounts of cumulus olivine (Jackson, 1961).

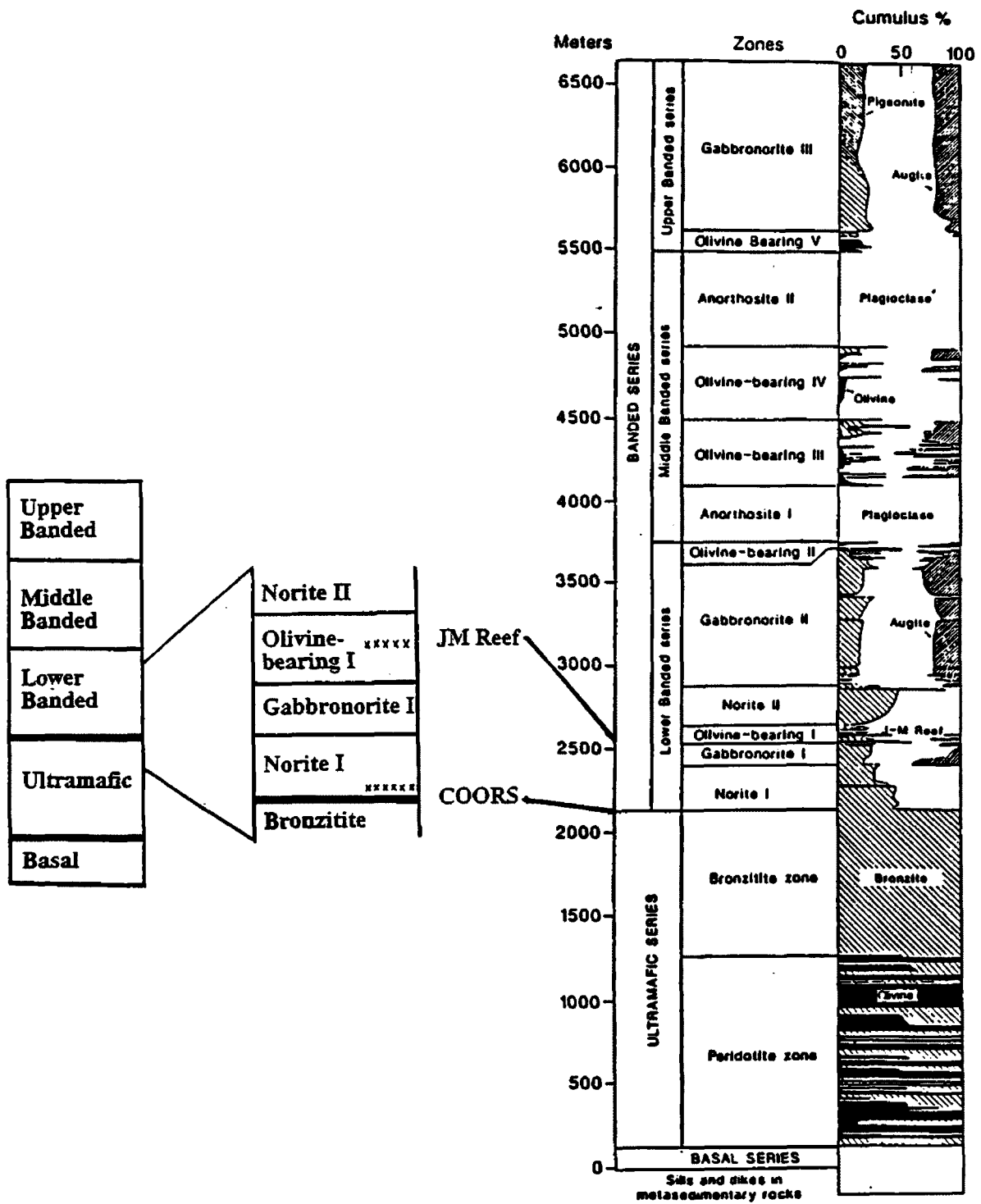


Figure 2. Stratigraphic subdivisions of the Stillwater Complex and approximate cumulus modal distribution (Zientek et al., 1985)



<b>Name</b>	<b>Cumulus minerals</b>	<b>Notation*</b>
Anorthosite	plagioclase	pC
Norite	plagioclase, low-Ca pyroxene	pbC
Gabbro	plagioclase, augite	paC
Orthopyroxenite (Bronzite)	low-Ca pyroxene (bronzite)	bC
Gabbronorite	plagioclase, low-Ca pyroxene, augite	pbaC
Dunite	olivine	oC
Olivine-bearing (Troctolite)	plagioclase, olivine	poC
Olivine gabbro	plagioclase, augite, olivine	paoC
Olivine gabbronorite	plagioclase, augite, low-Ca pyroxene, olivine	paboC

Table 1. Terminology for describing rocks of the Stillwater Complex. C = cumulate; p=plagioclase; b=low-Ca pyroxene; a = augite; o = olivine. In the shorthand notation, cumulate phases are listed in order of abundance. (modified from Page, 1977)

The Ultramafic Series is subdivided into the Peridotite Zone and the Bronzite Zone. The repetitive cycles of the Peridotite Zone, have been extensively studied (Jackson, 1961; Irvine, 1980; Howland, 1955; Raedeke and McCallum, 1984; and others). Characteristic cycles contain a sequence of dunite, dunite and chromite, harzburgite, and bronzite. Not all layers are present in every cycle.

Because of its uniform composition, the Bronzite Zone has been studied by only a few workers (Raedeke and McCallum, 1984; Todd et al., 1982; McCallum et al., 1980), and not much detailed work has been done. The contact between the Peridotite Zone and the Bronzite Zone is marked by the upward disappearance of cumulus olivine. The Bronzite Zone makes up approximately the top one-third of the Ultramafic Series, and consists of cumulus orthopyroxene, intercumulus plagioclase, and commonly augite oikocrysts. Thin olivine-bearing and chromite-rich layers are found in the bronzite, near the upper contact (Todd et al., 1982). The amount of intercumulus plagioclase increases towards the top of the Bronzite Zone until it also becomes cumulus; thereby marking the contact with the Norite I Zone of the Lower Banded Series (McCallum et al., 1980).

The remaining three-fourths of the Stillwater Complex, the Lower, Middle, and Upper Banded Series, overlies the previously mentioned units. These Series, mainly plagioclase-bronzite cumulates, plagioclase-bronzite-augite cumulates, plagioclase-olivine cumulates troctolites, and plagioclase cumulates, are subdivided into 12 zones (McCallum et al., 1980).

Numerous studies exist on the Lower Banded Series since it hosts the PGE-bearing sulfides (Irvine et al., 1983; Campbell et al., 1983; Naldrett, 1990; Bow et al., 1982; Todd et al., 1982; Page and Moring, 1990). The Lower Banded Series consists of the Norite I and Gabbronorite I zones, the Olivine-bearing I Zone, which hosts the PGE-rich sulfides known as the JM Reef, the Norite II, Gabbronorite II, and Olivine-bearing II zones (McCallum et al., 1980).

The Norite I Zone consists of layers of plagioclase and bronzite, and cumulates with variable amounts of each. The upper contact with Gabbronorite I is marked by the first occurrence of cumulus augite above the Basal Series (Zientek et al, 1985). The overlying Gabbronorite I Zone consists of plagioclase, bronzite, and augite cumulates, all of which vary in proportion (Zientek et al, 1985).

Olivine-bearing I Zone begins at the reoccurrence of cumulus olivine. This unit contains olivine, plagioclase, bronzite, and augite cumulates as well as pegmatoids (Zientek et al, 1985, McCallum et al., 1980; Raedeke et al., 1985). Many of the olivine-bearing units contain less than five percent cumulate olivine (McCallum et al., 1980). The one to three-meter PGE-bearing JM reef is generally located near the fifth olivine-bearing unit at the base of the anorthosite and the top of the troctolite. The location of the JM reef varies somewhat along strike, but is found approximately 400 to 450 meters above the contact between the Banded and Ultramafic Series (Todd et al., 1982). The upper contact of Olivine-bearing Zone I is between a plagioclase cumulate and a thick plagioclase, bronzite cumulate known as the Norite II (McCallum et al., 1980,

Zientek, 1985). The uppermost unit of the Lower Banded Series, Gabbronorite II, consists of layers of plagioclase, bronzite, augite cumulates and plagioclase cumulates. The reoccurrence of olivine marks the upper contact with Olivine-bearing Zone II, the uppermost layer of the Lower Banded Series.

The remaining Middle and Upper Banded Series consist of Anorthosite I, Olivine-bearing III, Olivine-bearing IV, Anorthosite II, Olivine-bearing V, and Gabbronorite III (McCallum et al., 1980). Zientek et al. (1985), describe these units in more detail.

## **PROBLEMS AND OBJECTIVES**

The Stillwater Complex contains several sulfide-bearing intervals, many of which are continuous along the strike of the complex (fig. 3). Only one such horizon, the JM reef, contains economic amounts of PGE's. PGE-bearing sulfides in layered mafic-ultramafic intrusions are typically found in such continuous horizons. However, some sulfide concentrations, as in the Lower Banded Series, are laterally discontinuous (Page et al., 1985). One of these concentrations, the Coors 602 zone, is primarily mineralized pegmatoidal bronzitites (Conn, 1979; Volborth and Housley, 1984). The study area is named Coors 602 zone after one of the exploration trenches in the area.

In 1967, the Johns-Manville Corporation began soil sampling and drilling to delineate the JM reef platinum horizon in the Stillwater (Conn, 1979). A detailed soil geochemical traverse across the Coors 602 zone showed significant PGE values (Conn,

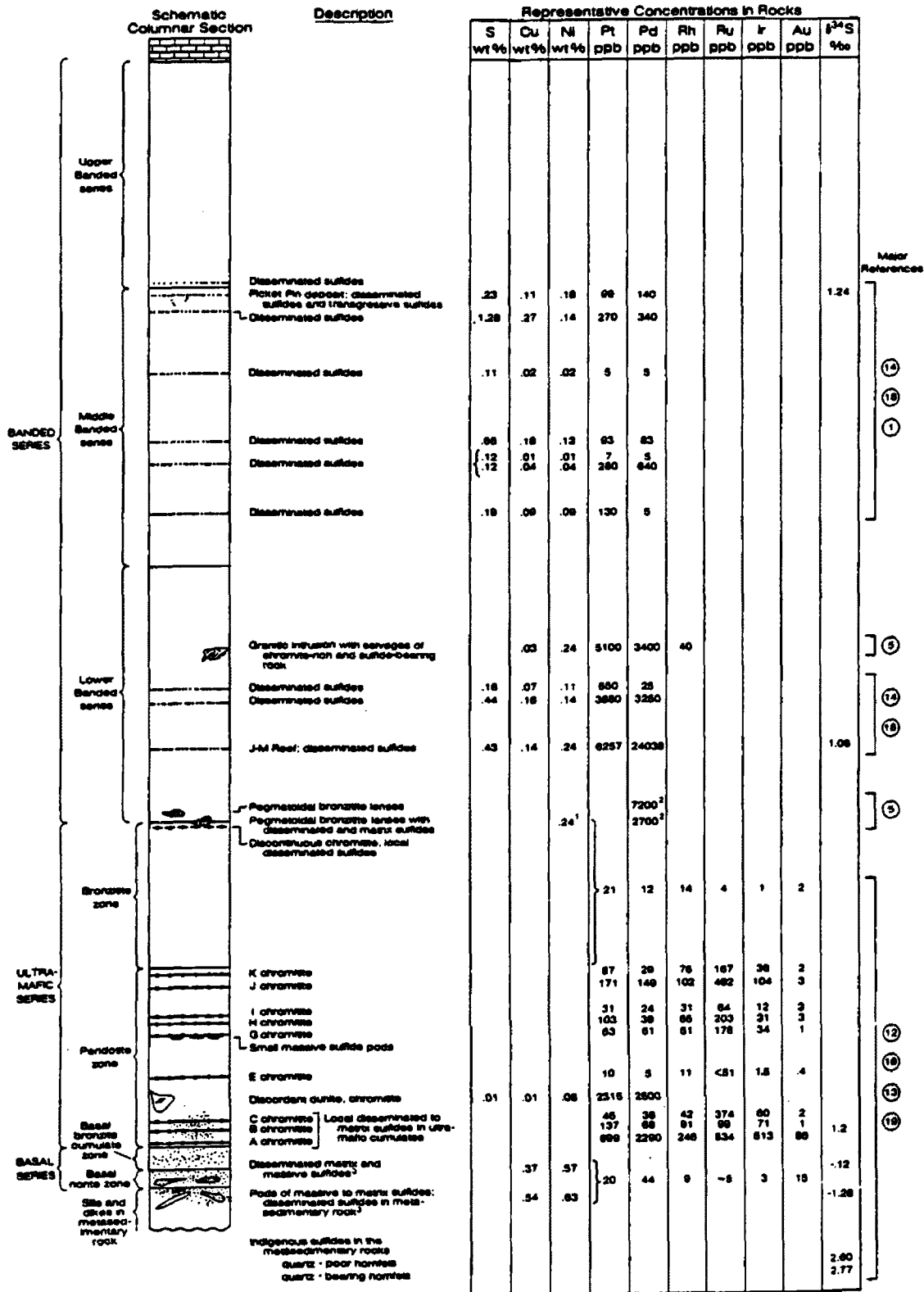


Figure 3. Schematic columnar section for the Stillwater Complex showing the relative locations of sulfide, platinum-group-element and chromite mineralization, and representative analyses of rocks. Footnotes: (1), combined Ni + Cu; (2), combined Pt + Pd; (3), based on rocks containing more than 50 percent visible sulfide (Page, et al., 1985).

1979). The anomalously high platinum values led to trenching and coring in the area in 1973 and again in 1982. When the richer PGE reef was discovered stratigraphically above the Coors 602 zone, exploration beneath ceased (S. Todd, pers. comm., 5/1991).

Although some of the platinum and palladium values exceed those of the JM Reef, the average value of these elements from the Coors 602 area is less than the JM Reef, and it is considered sub-economic. However, it is important to understand how and why mineralization occurred at this location. Although the Coors 602 zone is not economic, this horizon in which it occurs may represent a potential target for exploration elsewhere in the Stillwater and in other intrusions.

The bulk of the mineralization occurs in pegmatoids of bronzitite composition. This feature is very odd in that the pegmatoids occur within the Norite I unit, well above the disappearance of bronzitite in the Ultramafic Zone below. Other interesting features in the surrounding rocks include the thinning of the Gabbronorite Zone I to virtual absence, and units crosscutting other units. Also in the Coors 602 area, the typical uniform layering is disturbed forming highly irregular contacts with adjacent layers. It seems more than coincidental that these mineralized pegmatoids are found within a small area with all of these other atypical features; thus they are likely related. A viable genetic model must account for all these features including the close proximity to the JM reef, plagioclase first appearing as a cumulus phase, occurrence of pegmatoids, presence of significant PGE-bearing sulfides, and the stratigraphic disturbances are present.

## **COORS 602 AREA**

### **LOCATION AND GENERAL GEOLOGY**

The Coors 602 zone is located on the East Boulder Plateau between the East Boulder River and Lost Mountain (Fig. 4). Johns-Manville geologists prepared a 1" to 100' outcrop map of the area between 1974 and 1991 (Fig. 5a, in Appendix 1). Figure 5 is a 1" to 100' copy of this map.

Stratigraphic units in the Coors area are similar to the rest of the Stillwater Complex, with rocks ranging stratigraphically from the Bronzite Zone of the Ultramafic Series up through the Lower Banded Series (Fig. 2). The Gabbro-norite I Zone is only partially represented. Cumulate lithologies of these units are, in general, mineralogically and petrologically similar to typical exposures of the respective units elsewhere in the complex. The contact in the Coors 602 zone is also interpreted to be the first occurrence of cumulate plagioclase.

The actual contact between the Bronzite Zone and the first norite does not occur in outcrop in any location in the Coors area. The inferred contact on the map in figure 5 is within a meter from the true contact in most places, and less than 0.5 meters in several locations. In other locations throughout the complex, for example the Mouat Mine Road, the contact is sharp on the scale of a single grain. Thus, the same contact in the Coors 602 zone is assumed to have a similar sharpness. The contact between norites and bronzites in the trenches is not transitional, but very sharp. The contact between Norite I and Olivine-bearing Zone I was not studied in detail. The Reef does not occur in the fifth

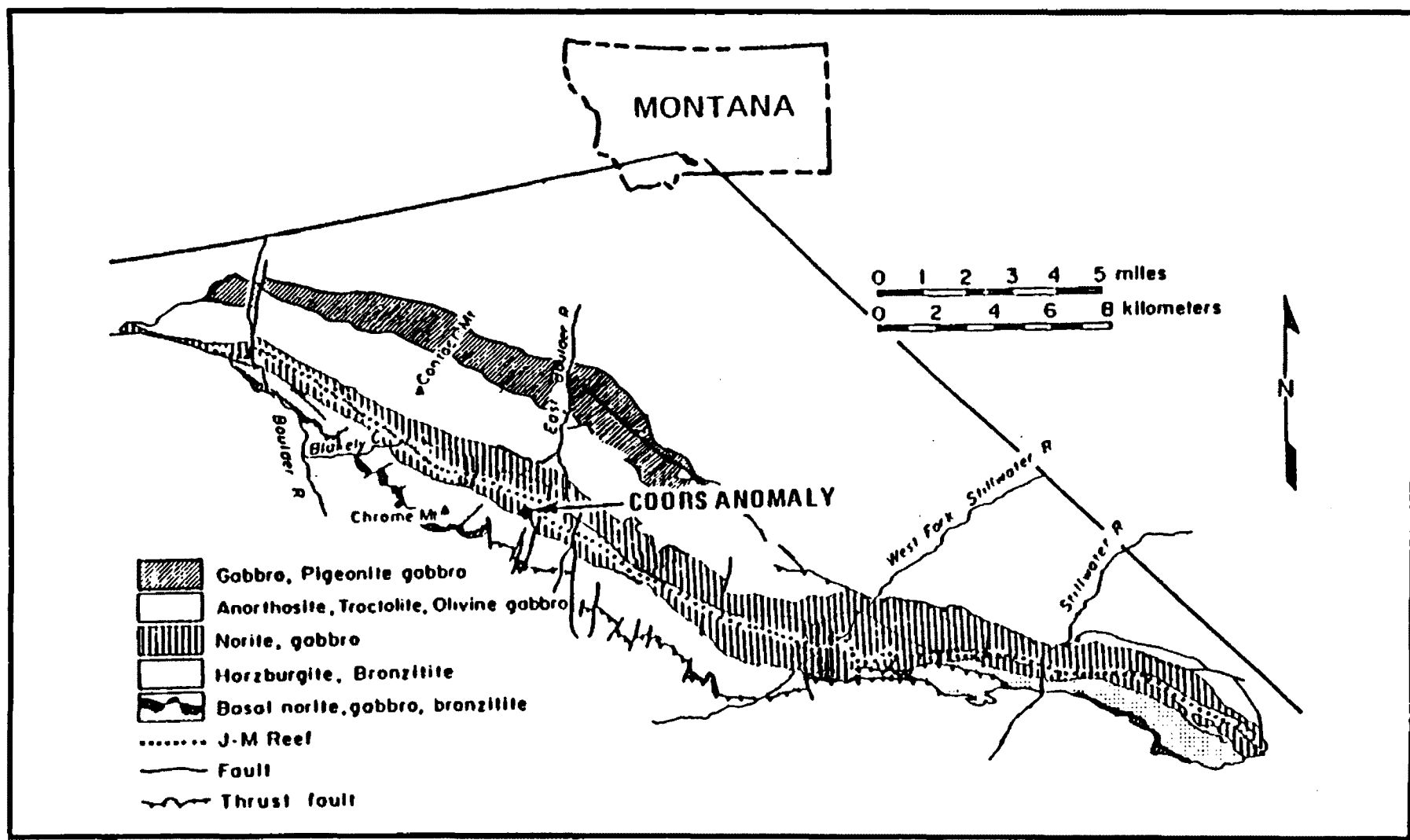


Figure 4. Simplified geologic map of the Stillwater Complex showing the location of the Coors anomaly (modified from Volborth, 1984)



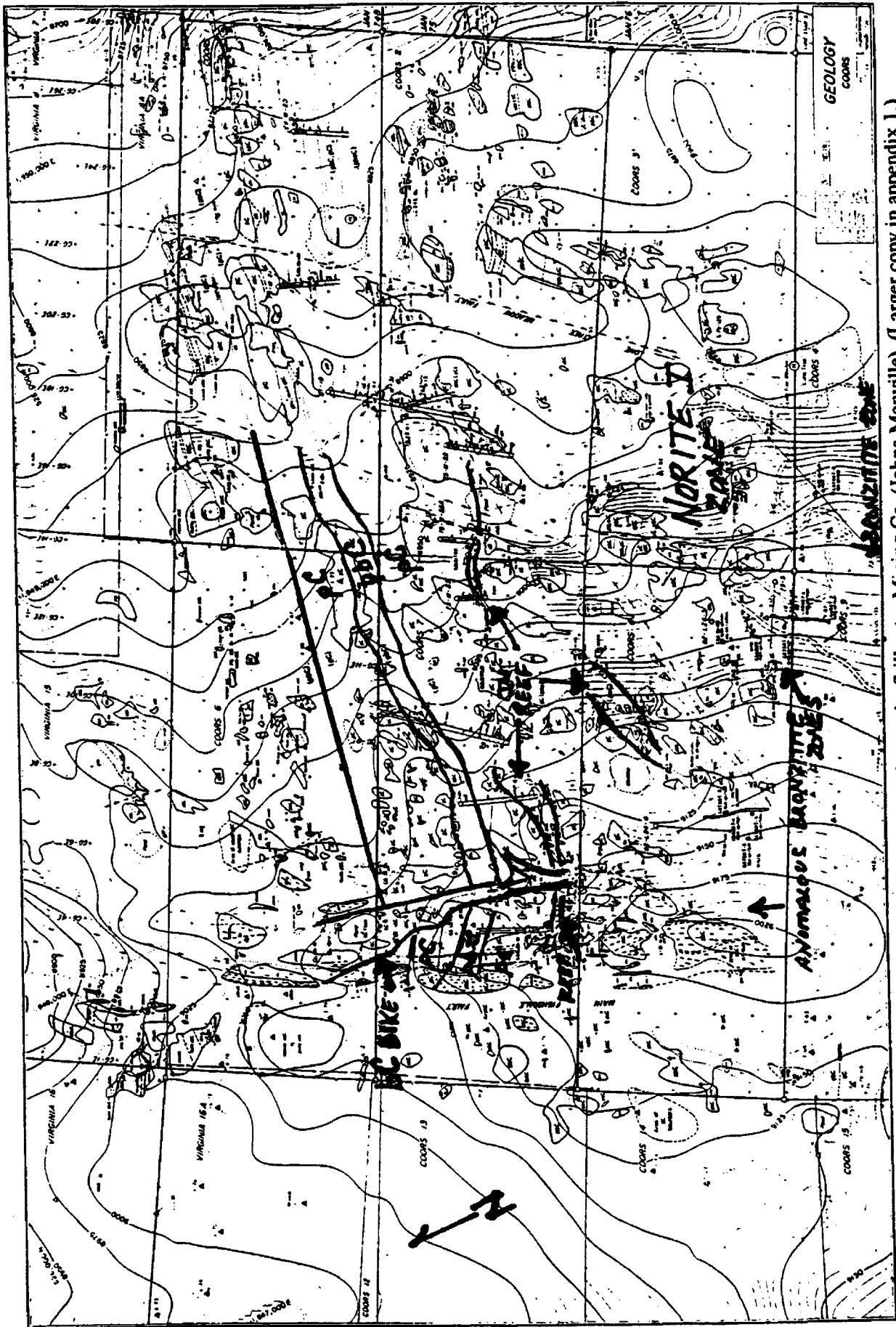


Figure 5. Outcrop map (1" = 400') prepared by geologists at the Stillwater Mining Co. (Johns-Manville) (Larger copy in appendix 1.)

olivine-bearing unit as it typically does throughout the Stillwater Complex. Instead, it occurs in the second or third olivine-bearing unit.

Although the Lower Banded Series in the Coors 602 area contains similar geologic units as are found in this Series throughout the Stillwater Complex, it displays many irregular relationships not typically seen in other locations. These irregularities are discussed in detail below.

## **METHODS**

Mapping for the current study was primarily reconnaissance of previously recognized geologic units, contacts, and structures in the area. The map produced by Johns-Manville was the basis for this work. Norite and bronzitite samples, both pegmatoidal and normal, were collected throughout the Coors area, mostly below the JM Reef (figure 6).

Geochemical and petrographic analyses were used to characterize the bronzitite masses, both mineralized and non-mineralized, to determine if they are similar to the bronzitite in the Ultramafic Series below and possibly originated from that unit. Due to the lack of previous research in the Bronzitite Zone of the Ultramafic Series, a suite of samples was collected from this zone along the Mouat Mine Road to add to the current sparse database for valid comparisons to the Coors 602 zone.

Thin sections were made from each sample collected and studied or petrographic description using a Zeiss polarizing-light microscope. Additional polished sections were

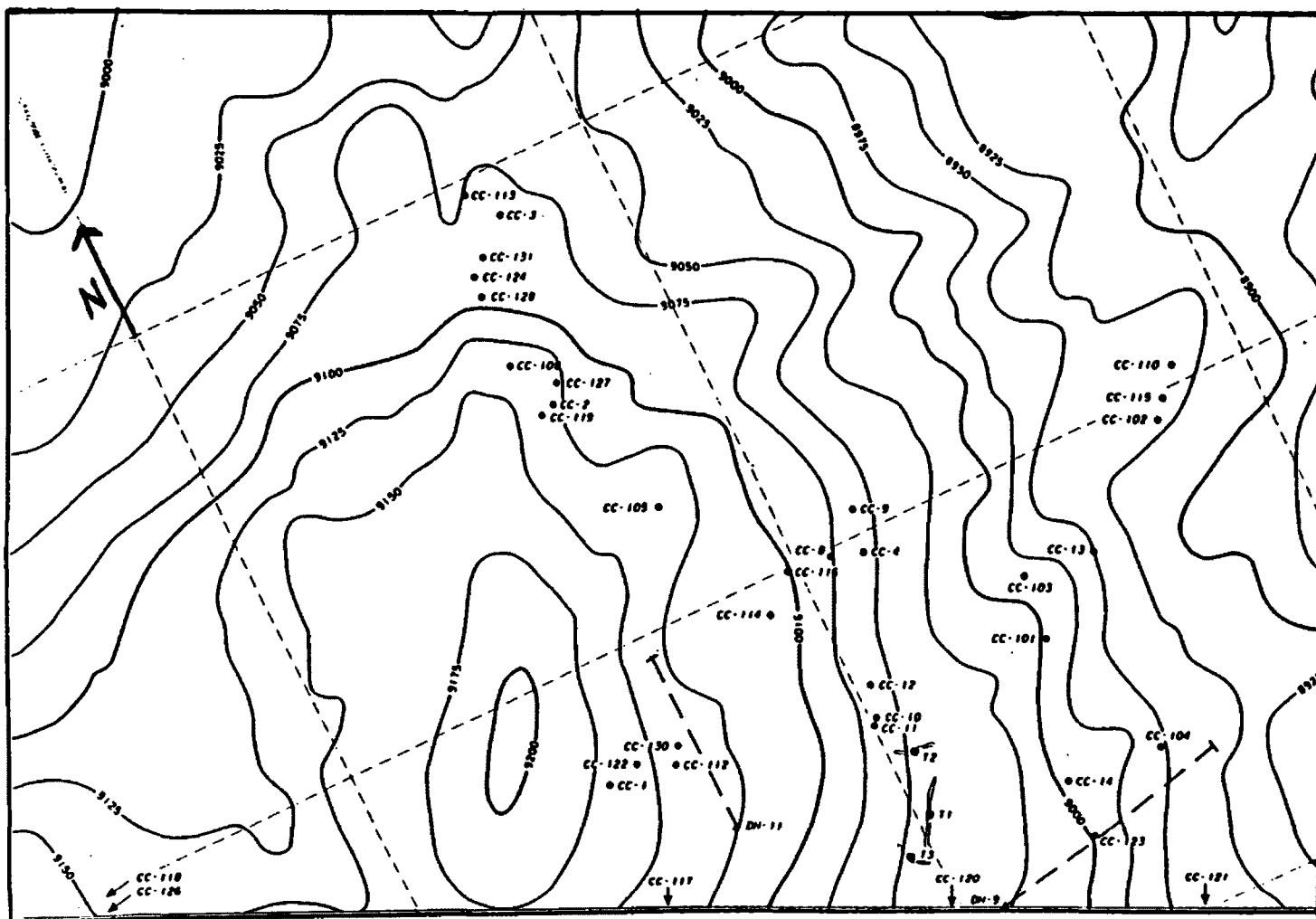


Figure 6. Sample location map (1"=400') from the Coors area. Note: use in combination with figure 5.

cut for examination under reflected light. Polished circular samples were cut and coated with carbon for microprobe analyses. Electron microprobe analyses were performed on bronzite grains from bronzitites of the Ultramafic Series, the bronzitites in the Coors 602 zone, and from norites within the Banded Series. The analyses were done on microprobes at both the University of Montana and Washington State University. The automated, wavelength dispersive, ARL-EMX five channel microprobe at the University of Montana was used at 15 KV accelerated voltage and 1 microampere of sample current. Washington State University's microprobe is also wavelength dispersive. The importance of these microprobe analyses was to determine the magnesium to iron ratio which can have a direct correlation to differentiation of the magma.

Representative samples were coarsely crushed and finely pulverized at the University of Montana. Powders were sent to The United States Geological Survey (USGS) in Denver and Washington State University for x-ray fluorescence (XRF) analyses. Numerous other analyses were done at the USGS in addition to XRF; these analyses are listed in table 2. Descriptions of these analytical methods can be obtained from the Denver office. Whole rock analyses were done to show whether the pegmatoidal samples or possibly the mineralized samples were formed from late-stage differentiates, thereby containing many incompatible elements. Magnesium and iron were used to compare differentiation trends.

<b>EDXRF</b>													
NB PPM	RB PPM	SR PPM	ZR PPM	Y PPM	BA PPM	CE PPM	LA PPM	CU PPM	NI PPM	ZN PPM	CR PPM		
<b>Optical Spectroscopy - ICP-AES, 40EL</b>													
	AL %-S	CA %-S	FE %-S	K %-S	MG %-S	NA %-S	P %-S	TI %-S	MN PPM-S	AG PPM-S	AS PPM-S	AU PPM-S	
	B PPM-S	BA PPM-S	BE PPM-S	BI PPM-S	CD PPM-S	CE PPM-S	CO PPM-S	CR PPM-S	CU PPM-S	EU PPM-S	GA PPM-S	GE PPM-S	
	HO PPM-S	LA PPM-S	LI PPM-S	MO PPM-S	NB PPM-S	ND PPM-S	NI PPM-S	PB PPM-S	SC PPM-S	SN PPM-S	SR PPM-S	TA PPM-S	
	TH PPM-S	U PPM-S	V PPM-S	W PPM-S	Y PPM-S	YB PPM-S	ZN PPM-S	ZR PPM-S					
<b>X-Ray Spectroscopy WDXRF Major Elements as Oxides</b>													
SIO2 %	AL2O3 %	FETO3 %	MGO %	CAO %	NA2O %	K2O %	TIO2 %	P2O5 %	MNO %	LOI 925C			
<b>AAHydride Generation</b>													
AS PPM	SE PPM												
<b>Graphite Furnace AAS</b>													
AU PPM													
<b>Chemical Separation Flame AAS</b>													
TE PPM													
<b>ICP Mass Spec.</b>													
PT PPB	PD PPB	RH PPB	RU PPB	IR PPB									
<b>Radiochemistry - INAA Long Count</b>													
FE %	NA %	BA PPM	CO PPM	CR PPM	CS PPM	HF PPM	RB PPM	SB PPM	TA PPM	TH PPM	U PPM	ZN PPM	
ZR PPM	SC PPM	LA PPM	CE PPM	ND PPM	SM PPM	EU PPM	GO PPM	TB PPM	TM PPM	YB PPM	LU PPM	CA %	
K %	AS PPM	AU PPB	NI PPM	SR PPM									
<b>FeO Potentiometric Titration</b>													
FEO %													
<b>Heat-weight loss H2O+-</b>													
H2O+ %	H2O- %												
<b>Coulometric titration Carb.C.</b>													
CO2 %													
<b>LIBO2</b>													
F %													
<b>Conway Cell</b>													
CL %													
<b>Infrared</b>													
TOTAL S%													

Table 2. USGS geochemical analytical methods including method used to analyze each element.

## **FIELD RELATIONSHIPS**

### **Bronzitite in Norite I**

Figure 5a shows the distribution of bronzitite in the Coors 602 area. Bronzitite occurs repeatedly upsection through the norite in the lower part of Norite I. Jones et al.(1960) report alternating layers at this contact elsewhere in the Stillwater, but extending only over a distance of about a meter into the Norite I. However, the bronzitites in the Coors 602 area randomly extend as much as 450 meters into the Norite I; they do not occur in layers. Exploration trench maps and drill logs both show these features. Refer to the figure 5a in appendix 1 or figure 6 for location of the trenches.

The thickness of the bronzitite masses zone ranges from only a few feet across to 100 meters, with respect to the longer axis of each. The shape of these bodies is difficult to discern given the lack of outcrop. The distribution and location of bronzitite is seen in the cores. Because only two of the cores intersect, the shape of the bronzitites is not evident. As seen in several outcrops, the bronzitites are discordant.

Small fractures are present, but there is no evidence of post-crystallization movement significant enough to have caused repetition of units as seen in the trenches. Since the bronzitite and norite alternate as frequently as every 3 meters over a 30 meter span, as seen in trench CG602T1, and no direct evidence of faulting was found, a faulting scenario is difficult to imagine. Other bronzitite outcrops are found just above this interlayered zone in sporadic locations throughout the Coors area.

In the western portion of the study area, along the Fishscale fault, bronzitite is found throughout a 360-meter vertical section beginning 60 meters above the approximate contact between the Ultramafic Series and the Banded Series (Fig. 5). Small patches of bronzitites are found throughout this fault zone up to the largest bronzitite outcrop at the north end. This large outcrop forms a lower contact with anorthosite, and occurs within the same outcrop as not only the anorthosite, but with a package of rock types including norite and troctolite. The units associated with this large bronzitite pod correlate with the adjacent stratigraphy, and have been moved only by rotation. This relationship suggests that the large bronzitite body was not displaced up section by post-crystallization faulting, but instead seems to have been magmatically emplaced. Most of the bronzitite outcrops are in place; however, it is questionable as to whether several of the small bronzitite outcrops have been relocated. They could be erratics moved from the Ultramafic Zone during glaciation. Although outcrops in the fault zone are scarce, the distribution of bronzitite is elongate and discordant and appears to be "dike-like."

Bronzitite rarely occurs above the Ultramafic Series in the Stillwater. In the Stillwater mine, many small (10 to 30 centimeters) ellipsoidal pods of orthopyroxenite are found 10 to 30 centimeters beneath the JM Reef. These pods beneath the JM reef are interpreted by Bow et al. (1982) as xenoliths from the Ultramafic Series.

Another occurrence of bronzitite in the Banded Series is in the Contact Mountain area. Pegmatoidal bronzitite pods as large as two meters occur along the contact of the

Olivine-bearing Zone I and the Gabbro-norite I, as well as within the Gabbro-norite I (Raedeke et al., 1985).

Drilling in Dow meadows, northeast of the Coors area, has documented another large bronzitite occurrence. The drill core goes through the reef, continues through normal stratigraphy below the reef, hits several meters of bronzitite, goes back into norite, and continues through bronzitite for the remainder of the hole. The core has been logged in detail, and the repetition of bronzitite is was not found to be a result of fault repetition (Zientek, pers. comm., April, 1993)

Secondary dunite in the Stillwater and Pt-rich dunite pipes in the Bushveld are examples of other discordant bodies found within different rock types. Although the composition of these bodies is quite different, similarities exist between them and the bronzitites.

The discordant dunites at Chrome Mountain lie stratigraphically beneath the Coors area. They crosscut cumulate layers approximately at right angles up through the Peridotite Zone on Lost Mountain. The secondary dunites, referred to as pipes in the Bushveld, are more predominant in regions of maximum faulting (Viljoen and Heiber, 1986).

### **Disturbed stratigraphy**

The stratigraphy overlying the Coors area is similar to the same horizon in the rest of the Stillwater. However, the stratigraphy below the reef in the Coors area is very



irregular. Layering between the reef and the Ultramafic Series contact with the Banded Series is disturbed and shows sinuous and highly irregular contacts (figure 5.). Many of the observed irregular contacts lie within the same outcrop, where it is clear that they were not produced by brittle deformation.

Norite I and Gabbronorite I typically contain irregular features (Foose, 1985). The thinner layers in Norite I often show scouring, slumping, and are laterally discontinuous. The upper portion of Norite I contains a laterally extensive layer exhibiting disturbed layering and irregular mixing of norite, anorthosite, and coarse-grained pyroxenite (McCallum et al., 1980). They suggest that such features could be the result of strong currents, slumping or both. Gabbronorite I also contains many irregular features such as graded layers, slumps, and the occurrence of inclusions of bronzitite that is texturally identical to that of the uppermost thirty meters in the Ultramafic Series (McCallum et al., 1980). In both units however, these irregularities are typically small, on the scale of centimeters, compared to the large discordances in the Coors area which may range across the entire study area (Fig. 5), a distance of about 2400 feet.

The disturbed layering described above for the Coors 602 zone generally occurs within the scale of one outcrop. However, discordant features also exist across the entire study area. An olivine-bearing pod occurs approximately 590 feet above the Bronzitite Zone, in the west part of the study area. This outcrop is interpreted to be the lower contact of the Olivine-bearing Zone I. The JM Reef above this olivine pod is about 885 feet above the Bronzitite Zone. The position of both of these units is well below the

average location in the Stillwater Complex for the first olivine-bearing unit, and the stratigraphic units below are unusually thin. In the east side of the study area, near Lone Tree Meadow fault, the reef is close to the average location in the Stillwater Complex at about 1375 meters above the Bronzite Zone (Fig. 5).

Several outcrops in the Coors 602 area contain discordant features, including the olivine-bearing pod described above, which are evidence of downcutting into the norite. One location in particular, contains truncated olivine-bearing and anorthositic layers against norite (Fig. 7).

The Stillwater mine has exposed a similar feature with the reef downcutting layering in the rocks below (Turner, 1985; Bow et al., 1982; Zientek, April, 1993, pers. comm.). The reef reaches to within 98 feet of the Bronzite Zone, and proceeds to cut upsection to its original position. The Gabbronorite I Zone varies in thickness throughout the complex, but not to the degree that it does in the Coors area. The Gabbronorite I Zone is virtually absent in the Coors area; augite-bearing rocks appear in very few samples.

An overall decrease in thickness in the stratigraphy between the Reef and the Bronzite Zone is present beginning as far east as the Janet 50 claims. Figure 8 shows the location of Janet 50 with respect to Coors 602. Janet 50 also contains mineralized bronzite pegmatoids. Detailed descriptions can be found in Volborth and Houseley, 1984. The association of both the Coors 602 and Janet 50 mineralized zones with thinning of the stratigraphy below the reef, may be significant. The

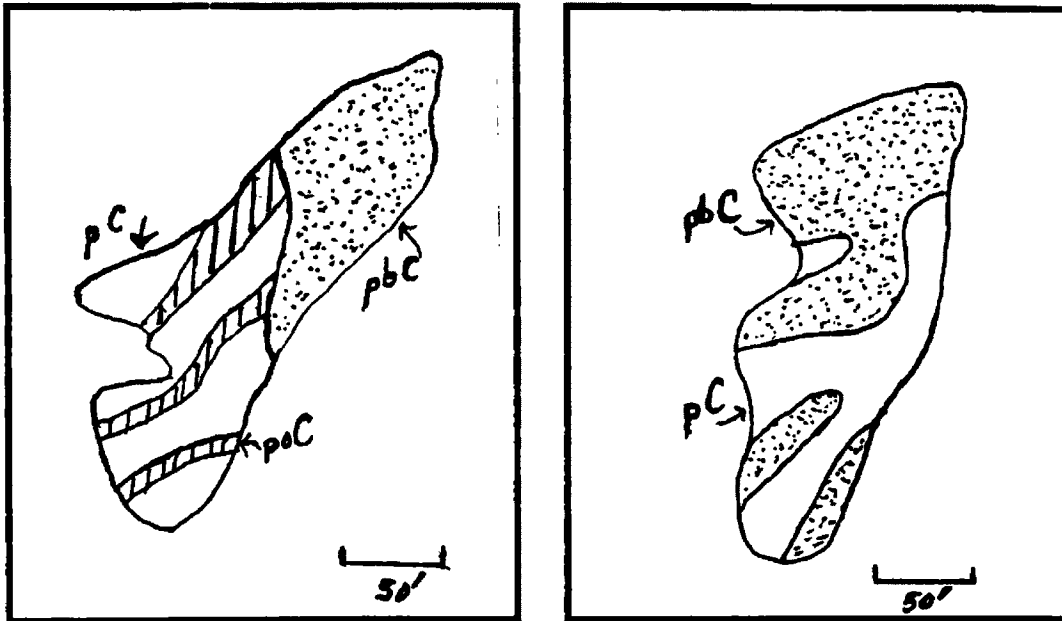


Figure 7. Sample outcrop sketches showing irregular layering and truncating features.

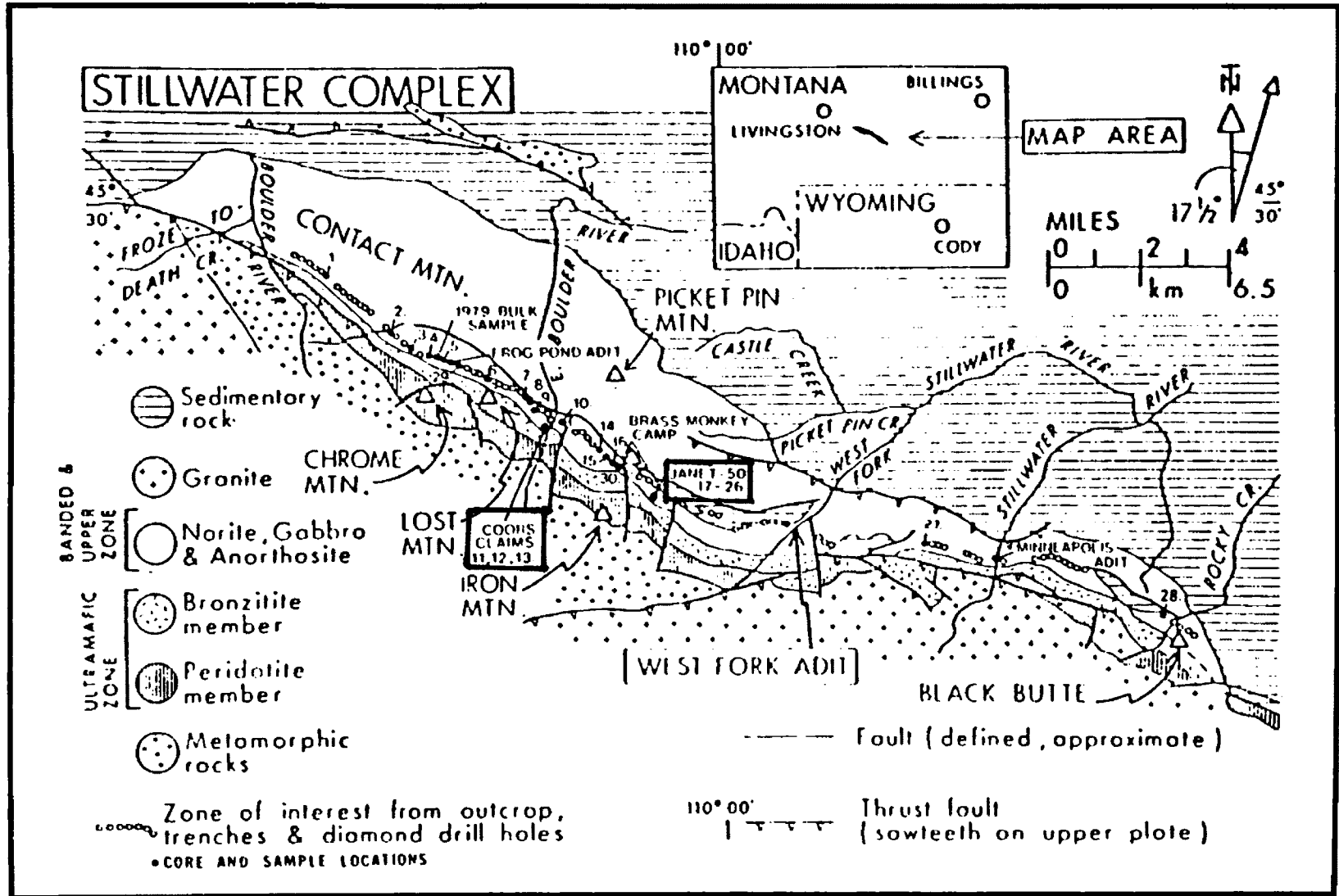


Figure 8. Geological map of the Stillwater Complex showing location of Janet 50 in relation to Coors 602.. (modified after Conn, 1979)

fact that the reef reaches lower than normal in these sites could be important in the genesis of the mineralization.

### **Pegmatoids**

Pegmatoids are widespread in layered intrusions. The term pegmatoid is preferred over pegmatite here because the latter typically refers to granitic composition.

Pegmatoid is a textural term referring to the coarse grain size, but the presence of volatiles, presumably water, can also be inferred. Pegmatoids occur in various rock types in layered intrusions, including chromitites, norites, bronzitites, troctolites, and gabbros; they have the same composition as the rock type in which they occur.

Most workers do not address the association between mineralization and pegmatoids. Pegmatoids commonly occur in both sulfide and chromite deposits. Pegmatoids are also found in areas of the Stillwater Complex which have no mineralization, as well as those associated with PGE mineralization. Many workers simply indicate that the pegmatoids are evidence for the presence of volatiles, not why the volatiles are there or where they came from.

In the Coors 602 area, rocks which have mineral grain sizes over the 5 mm are considered pegmatoids. Grain sizes range from approximately 5 mm to 150 mm. Pegmatoidal textures are found in both bronzitites and norites in the Coors 602 zone. Several pegmatoid patches of various sizes exist near the contact between the Ultramafic and Banded Series and elsewhere in the Lower Banded Series in the Coors 602 area.

Contacts in the trenches between pegmatoids and adjacent rock units are presently difficult to find due to collapse and weathering in the trenches. Where it was somewhat exposed, the contact seemed gradational over several centimeters. One contact observed between norite pegmatoid and bronzitite, in the CG789T-2 trench, is gradational over 15 cm.

Pegmatoids associated with the JM Reef contain a significant amount of phlogopite and thus water at magmatic temperatures; whereas those along the contact between the Banded and Ultramafic Series in the Coors area do not. Only a few pegmatoids sampled in the Coors area contained phlogopite. Bronzitite pegmatoids in the Coors 602 area, however, are unusual because they occur within norites.

### **PGE Mineralization**

Many of the bronzitites in the Coors 602 area contain PGE mineralization. Trenches dug by Johns-Manville help delineate the mineralized rocks. Both pegmatoids and nonpegmatoids contain mineralization. Sulfides appear to be randomly distributed throughout the bronzitites. Most of the mineralization is within the bronzitites in the lower Norite I. One bronzitite outcrop in the Fishscale fault zone contains significant proportions of sulfide mineralization. The large bronzitite at the top of the fault zone, does not contain appreciable sulfide mineralization. However, the rocks here are extremely sheared and altered, so any sulfides that were present may have been remobilized.

## **MINERALOGY AND PETROGRAPHY**

Sample descriptions including rock type, grain size of cumulate bronzite, and approximate percent orthopyroxene and sulfides are located in table 3.

### **Bronzitite**

The orthopyroxenites of the Bronzitite Zone are mineralogically and texturally similar to those elsewhere in the Stillwater. Euhedral to subhedral bronzite is the cumulate phase with augite and plagioclase as intercumulate phases. Augite is present as exsolution blebs and lamellae in bronzite crystals, as oikocrysts, and less commonly as intercumulus grains. Bronzite grains range from 2 to 5 mm in diameter. Augite oikocrysts range from 0.5 to 2 cm in diameter. Plagioclase grains, typically anhedral and interstitial, are not zoned. Modal proportions of minerals are 95 to 80% bronzite, 5 to 15% plagioclase, and 1 to 5% augite.

The bronzitite cumulates in the trenches and elsewhere in the Norite I Zone are quite different texturally from those in the Bronzitite Zone. Many bronzitites do not exhibit the normal cumulate texture and may be affected by recrystallization. Although bronzite must be the cumulate phase, it is often anhedral; it is difficult to discern whether it is actually cumulate. Similarly, it is difficult to tell if the plagioclase is intercumulus. Many samples seem to be marginally bronzitite and possibly could be norites. The plagioclase content in these bronzite cumulates ranges from 5% to 30%.

Cu	Ni	Pt	Pd	Pd/Pt	type	plg	sulf	size (cm)	peg
<b>C036T-1</b>									
150	284	125	130	1.04	pbC	35-45		.3-.5	
232	272	75	115	1.53	pbC	50		0.3	
257	285	85	85	1.31	pbC	30-60	tr-1	.3-.5	
184	225	100	95	0.95	pbC	60-70	tr-5	.3-.5	
142	230	50	85	1.30	pbC	60-70	tr-5	.3-.5	
72	320	<50	50		pbC	50	tr	.5-1.5	p
80	450	<50	85		bC	10-30	tr-1	.3-.5	
372	500	425	380	0.89	bC	10-30	tr-1	.3-.5	
372	490	525	555	1.08	bC	10-30	tr-1	.3-.5	
435	580	425	1,250	2.94	bC	10-30	tr-1	.3-.5	
800	550	700	515	0.74	bC	10-15	1	0.3	
289	595	575	455	0.79	bC	10-15	1	.5-.7	
880	1,075	450	410	0.91	bC	<5	1	0.5	
370	480	850	550	0.85	bC	10-15	1	0.5	
740	870	900	800	0.87	bC	10-20	tr-5	.5-1.5	p
920	1,250	800	950	1.19	bC	10-20	3-5	.5-1.5	p
420	475	550	430	0.78	bC	10-20	3-5	.5-1.5	p
910	1,085	925	800	0.88	bC	10	1-3	.5-1.5	p
530	600	775	750	0.97	bC	10-20	1-5	.5-1.5	p
255	380	150	130	0.87	bC	10-20	1-5	.5-1.0	p
316	450	75	70	0.93	bC	10-20	1-5	.5-1.0	p
405	570	175	130	0.74	pbC	50-60		.5-1.0	p
38	103	<50	20		pbC	50-60		.5-1.0	p
17	85	<50	20		pbC	50-60		0.5	
14	70	<50	25		pbC	50-60		0.5	
14	54	<50	25		pbC	50-60		0.5	
18	80	50	25	0.50	pbC	50-60		0.5	
178	390	300	245	0.82	bC	20-35	tr-2	.1-.5	
190	340	200	245	1.23	bC	20-35	tr-2	.1-.5	
182	330	200	220	1.10	bC	20-35	tr-2	.1-.5	
188	295	200	170	0.85	bC	20-35	tr-2	.1-.5	
380	430	500	300	0.80	bC	20-35	tr-2	.1-.5	
352	485	500	325	0.85	bC	20-50	1-2	.3-.4	
49	98	100	80	0.80	pbC	60-70		.3-.4	
18	52	50	30	0.80	pbC	60-70		.3-.4	
12	50	50	25	0.50	pbC	60-70		.3-.4	
<b>C002T-2</b>									
289	325	850	1,700	2.82	bC	10	tr	<3	peg
116	188	150	180	1.20	pbC	50-60	0-5	0.4	
324	300	1,400	3,700	2.84	bC	10	tr-5		peg
385	380	875	1,800	2.87	bC	10	tr-5		peg
500	425	325	595	1.83	bC	10	tr-5	<3	peg
53	200	<50	45		pbC	60			
22	212	<50	70		pbC	60	0		
98	212	50	60	1.20	pbC	60			
224	385	350	1,000	2.88	bC	20	tr-5	.5-1	peg
590	520	2,700	9,000	3.33	bC	20	tr-5	.5-1	peg
435	440	800	2,500	3.13	bC	20	tr	<2	peg
292	324	300	425	1.42	bC	20	tr	<2	
164	220	100	120	1.20	bC	<5	tr	.2-.7	
142	200	125	100	0.80	bC	<5	tr	.8-.7	
144	212	125	90	0.72	bC	<5	tr	.2-.7	
58	164	75	80	1.07	pbC	60		.3-.5	
18	54	75	55	0.79	pbC	60		.3-.5	
20	54	50	75	1.50	pbC	60		.3-.5	
<b>C002T-1</b>									
580	700	1,800	2,750	1.72	bC	20	tr	<1.5	peg
158	190	100	145	1.45	bC	20	tr-1	.3-.8	
88	138	50	85	1.70	pbC	40	tr	.1-1.0	peg
173	232	75	225	3.00	pbC	40	tr	.1-1.0	peg
130	188	50	75	1.50	pbC	40	tr	.1-1.0	peg
128	242	100	395	3.95	pbC	40	tr	.1-1.0	peg
233	405	600	2,200	3.67	bC	20	tr-5	1-1.5	peg
875	490	3,800	9,200	2.58	bC	20	tr-5	1-1.5	peg
460	505	2,250	6,400	2.84	bC	20	tr-5		
228	384	150	600	4.00	bC	20	tr-5		
80	110	50	80	1.80	pbC	40-50		.3-1	peg
158	180	50	80	1.80	pbC	40-50		.3-2	peg
285	380	400	1,200	3.00	pbC	40-50		.3-3	peg
280	338	400	1,400	3.50	pbC	40-50		.3-4	peg
480	375	1,050	4,000	3.81	bC	20-30	tr-1	1-1.5	peg
344	350	550	1,700	3.09	bC	20-30	tr-1	1-1.8	peg
382	400	325	1,700	5.23	bC	20-30	tr-1	1-1.7	peg
805	480	8,200	11,000	1.77	bC	20-30	tr-1	1-1.8	peg
855	620	8,800	13,000	1.91	bC	20-30	tr-1	1-1.9	peg
1,850	1,450	14,800	34,000	2.33	bC	5	tr-5	1-1.5	peg
450	430	1,450	5,500	3.79	bC	20	tr	1	peg
440	385	1,450	4,700	3.24	bC	20	tr	1-2	peg
87	162	50	105	2.10	pbC	50-60		.3-.5	
50	138	50	85	1.30	pbC	50-60			
72	118	300	820	2.07	pbC	50-60			
28	80	50	40	0.80	pbC	50-60			
28	88	50	25	0.50	pbC	50-60			
252	336	200	280	1.40	bC	20	tr	1	peg
292	385	425	1,000	2.35	bC	20	tr	1	peg
<b>C002T-3</b>									
38	85	<50	20		pbC	80			
32	70	<50	25		pbC	80		.3-.4	
180	380	<50	55		bC	5-25	0-tr		
249	570	100	210	2.10	bC	5-15	tr-5	<1	peg
242	445	150	330	2.20	bC	10	1	<1	peg
338	750	200	435	2.18	bC	<1		<1	peg
144	340	50	80	1.80	bC	10-20		.5-2	peg
300	440	200	275	1.38	bC	10-20	0-tr	<3	peg
460	575	325	400	1.23	bC	5	0-tr		
200	380	250	800	3.20	bC	5	0-tr		
352	510	2,800	8,900	2.48	bC	5	0-tr		
1,280	1,150	10,000	28,000	2.80	bC	5	0-tr	1	peg
1,350	1,550	5,550	22,000	3.98	bC	5	5-10		
850	875	3,050	5,500	1.80	bC	5	tr-2	<2	peg
480	495	200	240	1.20	bC	10-20	tr-2	.2-1.2	peg
580	685	325	350	1.08	bC	10-20	tr-2	.2-1.2	peg
840	780	350	420	1.20	bC	10-20	tr-2	0.5	
388	400	350	820	1.77	bC	10-20	tr-2	.2-1.2	peg
<b>Pd/Pt Avg = 1.77</b>									

Table 3. Sample description including rock type, grain size, percent orthopyroxene, and approximate percent sulfide. Shorthand notations include: mm=Mouat Mine; cc=Coors Claim; T1, T2, T3=trench 1,2,3 respectively; 8,9,11=drill core 8,9,11 respectively.



## **Norite**

The Norite I Zone contains anhedral to subhedral cumulus plagioclase and bronzite, with interstitial augite. Augite, as in the Bronzite Zone, forms lamellae and blebs in orthopyroxene, and oikocrysts. The exsolved blebs are more abundant in the Norite I Zone compared with the Bronzite Zone. Augite also forms incomplete rims on some of the bronzite. Excluding the pegmatoidal samples, the bronzite ranges from 2 to 5 mm, the plagioclase from 1 to 5 mm. Where plagioclase is within an augite oikocryst, the grains tend to be small laths, 0.1 to 1 mm long. Rounded plagioclase grains can be found in bronzite, and bronzite grains in plagioclase. Some samples show slight to extreme embayment of both types of grains. The possibility that resorption caused the embayment is discussed below.

## **Sulfides**

In the Coors area, sulfides are commonly found as discrete grains interstitial to or within cumulus orthopyroxenes. Sulfides are also found along cleavage fractures in bronzites. Sulfides are more abundant in bronzites than norites, and they occur within both pegmatoidal and nonpegmatoidal rocks. The distribution of sulfide mineralization is podlike and highly irregular. Chalcopyrite, pyrrhotite, pentlandite, and pyrite are intergrown in blebs and disseminated grains and seem to have formed from an immiscible sulfide liquid. Sulfide blebs range in grain size from a fraction of a millimeter to a centimeter. Total sulfides range from 0.5% to 5%; the average is 2.

Economic reserves of PGE mineralization in the Stillwater are confined to the JM Reef. The PGE mineralization is associated with sulfides, predominantly pyrrhotite, pentlandite, chalcopyrite, and various PGE minerals (Bow et al. 1982). There is a direct correlation with the amount of sulfides and the PGE value in all rocks assayed

### **Alteration**

The most common alteration mineral is serpentine. Serpentine and chlorite occur as veinlets and replacement material within bronzites. Plagioclase alters to saussurite and clinzoisite. Actinolite often occurs as acicular crystals in and around sulfides.

### **Resorption**

Many of the rocks studied, especially norites and plagioclase-rich bronzitites, show slight to intense embayments of bronzite. Orthopyroxenes in the plagioclase-rich bronzitites also show a texture that could be attributed to slight remelting of the cumulates. The bronzites contain irregularly shaped inclusions of plagioclase which seem to have formed in preexisting depressions or embayments. Several reasons why resorption might occur, include temperature increase, load-pressure decrease, and addition of lower-temperature constituents or volatiles (fig. 9).

Temperature increase may result from either a pulse of new magma injected at slightly higher temperatures, or settling of crystals into a hotter melt. Assuming the

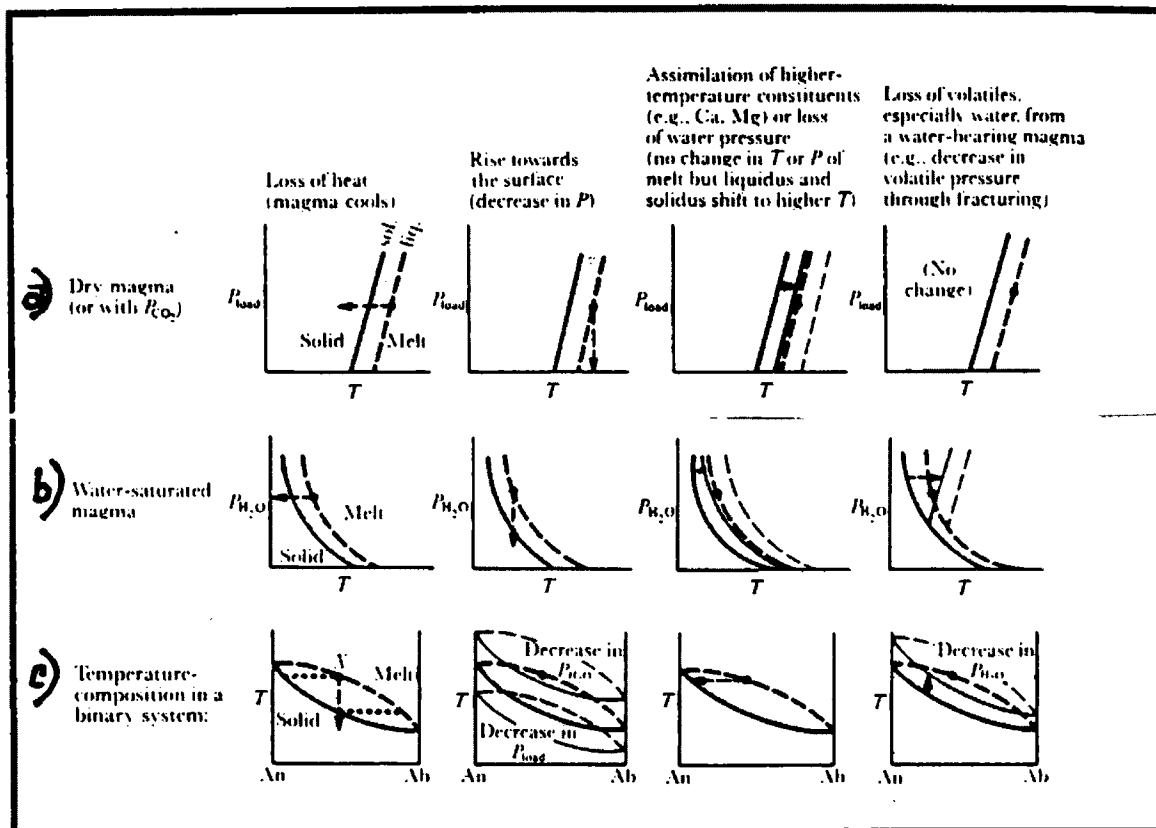


Figure 9. a) Pressure - temperature diagrams for a dry magma and b) a water undersaturated magma. c) temperature-composition diagrams for a binary system (modified from Hyndman, 1985, p. 100). In most instances, shifts discussed are opposite to those shown.

composition of the crystallizing magma in both cases was similar to that from which the bronzite formed, heating would cause melting of crystals (Fig. 9a). Textural evidence and microprobe analyses of resorbed grains do not indicate any adcumulus growth or further crystallization of bronzite with continued cooling. One possibility is that the Mg-Fe diffusion rate in bronzite was high. Alternatively, either the bronzite constituents which went into the melt during resorption were later separated from the interstitial melt before crystallization or the interstitial melt composition was changed with bronzite no longer on the liquidus.

Resorption textures could also result from a decrease in load pressure to initiate remelting (Fig. 9b). This could be accomplished by mechanical means such as fracturing within the crystallized part of the complex. Lipin (1992), suggested that the Stillwater magma erupted many times during formation. Such an event would cause a pressure decrease over the entire complex, and the resorbed grains should be a common feature for that entire horizon in which they are found.

If low-temperature components were added, possibly by upward migration of more differentiated melt, and mixed with the interstitial fluid of the crystallizing magma, the composition would shift, causing instability of pyroxene crystals (Fig. 9c). Such new constituents could have been introduced by one or more pulses of magma.

Addition of water could also cause resorption. Carbon dioxide has a similar but much lesser effect. Such volatiles could have been added to the resorbed area, by movement of late-stage volatiles concentrated from another crystallizing area, or from

country rocks being metamorphosed below the intrusion. The effect is similar to addition of other low-temperature constituents (Fig. 9d); it would lower the liquidus temperature. The lower liquidus places the orthopyroxene crystals out of equilibrium; thus resorption occurs.

Embayed grains may be explained by surface energies. Two minerals with different composition have different surface energies. When the two are touching, the mineral with the highest surface energy dominates the crystallization pattern (Spry, 1979). As a result, the mineral with the highest energy seems to be protruding into the other mineral, thus producing an embayed margin in the latter. This can account only for some of the embayed textures seen in the bronzitites from the Coors-602 area. Other embayed textures are difficult to explain by this model.

## **GEOCHEMISTRY**

### **Silicate**

Microprobe analyses for bronzitites in the Coors area are given in table 4. The Bronzite Zone in the Stillwater Complex shows little chemical variation vertically; the Mg numbers ( $Mg/Mg+Fe$ ) for orthopyroxene vary by only a few percent (Raedeke and McCallum, 1985 and Lambert, 1982). Lambert's data (1982) contain a few Mg enrichment zones which may indicate reversals, but they are not as pronounced as in the Peridotite Zone below. Orthopyroxenes from two locations in the Bronzite Zone, the Coors and the Mouat Mine area, were analyzed by electron microprobe for Si, Al, Ca,

**Electron Microprobe Analyses of Orthopyroxene from Coors Area (wt %)**

sample #	SiO <sub>2</sub>	CaO	Al <sub>2</sub> O <sub>3</sub>	FeO	MgO	Cr	TiO <sub>2</sub>	Ni	MnO	Total
mm-0	55.72	1.73	1.37	10.35	31.09	NT	NT	NT	NT	101.51
mm-50	56.18	2.23	1.30	10.25	30.14	NT	NT	NT	NT	101.06
mm-510	55.97	1.54	1.41	11.12	30.05	0.44	0.16	0.05	0.21	100.48
mm-588	55.91	1.82	1.41	12.38	28.58	NT	NT	NT	NT	101.64
mm-C	55.85	0.90	1.28	10.52	31.02	0.45	0.15	0.07	0.24	100.47
cc-2	54.44	12.07	1.64	10.81	20.22	NT	NT	NT	NT	98.19
cc-3	57.32	1.53	1.37	12.18	29.39	NT	NT	NT	NT	102.31
cc-8A	55.55	1.39	1.33	11.67	30.20	NT	NT	NT	NT	100.37
cc-10	54.19	1.63	1.45	14.46	27.29	NT	NT	NT	NT	98.63
cc-12	55.02	1.08	1.32	14.91	27.67	0.27	0.11	0.07	0.29	100.72
cc-104	55.20	1.04	1.09	12.68	29.20	0.31	0.20	0.07	0.26	100.06
cc-110C	55.46	1.14	1.28	12.43	29.37	0.16	0.16	0.08	0.25	100.33
cc-112	54.64	1.38	1.28	15.06	27.16	0.28	0.26	0.10	0.25	100.40
cc-115	56.04	1.26	1.15	11.58	29.98	0.31	0.16	0.08	0.27	100.83
cc-117	54.82	1.77	1.33	10.58	29.93	0.42	0.22	0.04	0.27	99.37
cc-120	55.14	2.14	1.36	10.89	29.86	0.61	0.19	0.06	0.26	100.48
cc-123	55.36	0.89	0.92	12.80	29.30	0.21	0.16	0.05	0.27	99.95
cc-130	53.52	0.84	1.28	14.07	27.02	0.22	0.15	0.07	0.25	97.42
T1-15F	55.70	1.43	1.43	11.64	30.00	0.30	0.11	0.09	0.24	100.94
T1-70	55.46	1.69	1.09	13.35	28.52	0.21	0.11	0.07	0.27	100.77
T2-23	55.54	1.36	1.19	15.45	26.54	NT	NT	NT	NT	99.33
T3-20	55.16	1.37	1.18	16.59	25.58	NT	NT	NT	NT	99.65
T3-85	54.70	2.44	1.38	13.61	27.32	0.26	0.13	0.07	0.32	100.22

Table 4. Electron microprobe analyses of orthopyroxene from the Coors area and Mouat Mine road given in weight percent. MM analyses done at WSU; cc and T analyses done at USGS.

Mg and Fe. Figure 10 is a plot showing Mg number ( $Mg/Mg+Fe$ ) trends. The data for this graph is listed in Table 5. The Mouat Mine samples begin roughly 200 meters below the contact between the Bronzite Zone and the Lower Banded Series. A decrease in Mg number from 0.84 to 0.80 towards the upper contact indicates the magma was becoming progressively more iron-rich probably as a result of magma differentiation. Only the top 600 feet of the Coors area were sampled and analyzed. McCallum (1980), cites  $Mg/(Mg+Fe)$  values of 0.84 at Chrome Mountain and 0.85 at Mountain View. McCallum suggest that the variation in these two sites may mark a lateral change in composition of the Bronzite Zone. However, the differences do not seem statistically significant.

A significant jump does occur, however, across the contact from the Ultramafic Series into the Banded Series at Coors. Mg numbers drop as much as thirteen percent, with all the lower values occurring in mineralized samples (group B in Fig. 10). Unmineralized bronzites and norites have bronzites with higher Mg numbers relative to the mineralized samples, even in samples higher up-section (groups C and E in Fig. 10). An exception to this is group D1 in Figure 10, with high Mg numbers, which are mineralized samples from the JM reef. Group D2 in Figure 10, with low Mg numbers are mineralized samples from the bC "dike"

XRF whole rock analyses for the Coors area are given in table 6. Samples show a decrease in  $Mg/(Mg+Fe)$  up section, indicating an increase in iron, similar to the bronzite microprobe analyses (Fig. 11). The data for this graph are listed in table 7. Again, similar to the probe graph, the mineralized samples (group B and D2 on Fig. 11) have the lowest

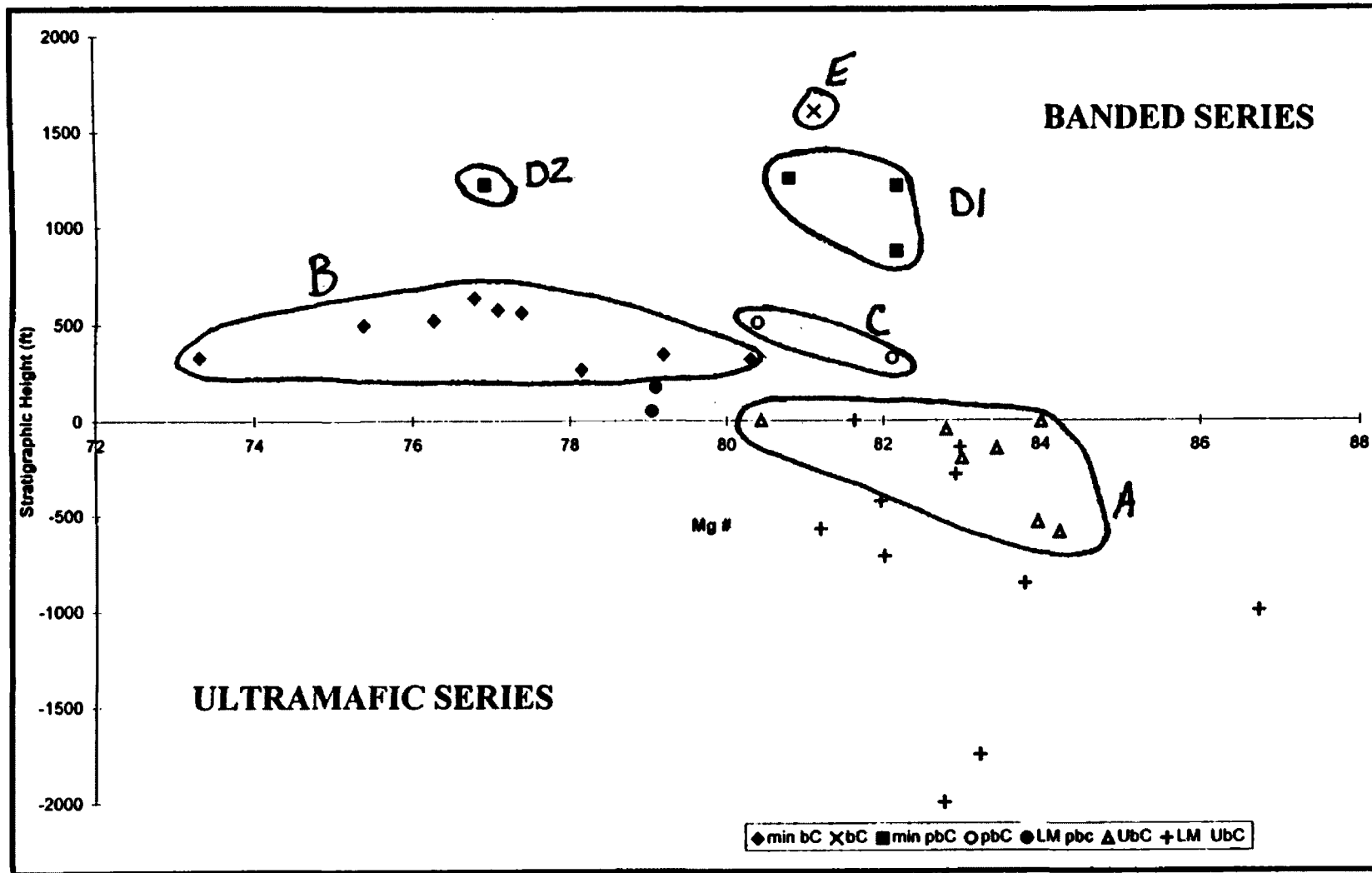


Figure 10. Plot of stratigraphic height versus magnesium number (mol percent Mg) of bronzite using the Banded Series - Ultramafic Series contact as the datum. Data is based on electron microprobe analyses of orthopyroxene. ("min" preceding rock type in legend box indicate mineralized samples.)



Sample #	Rock Type	mol% Mg	Height
mm-0	UbC	84.25	-588
mm-50	UbC	83.97	-538
mm-510	UbC	82.80	-50
mm-588	UbC	80.45	0
mm-C	UbC	84.01	-10
cc-2	pbC	76.92	1215
cc-3	bC	81.13	1605
cc-8A	poC	82.17	870
cc-10	pbC	77.08	575
cc-12	bC	76.78	635
cc-104	pC	80.40	510
cc-110C	pbC	80.81	1250
cc-112	bC	76.26	520
cc-115	pbC	82.18	1210
cc-117	UbC	83.45	-150
cc-120	UbC	83.01	-200
cc-123	bC	80.31	320
cc-130	bC	77.38	560

Sample #	Rock Type	mol% Mg	Height
T1-15F	pbC	82.11	325
T1-70	bC	79.19	345
T2-23	bC	75.38	495
T3-20	bC	73.31	330
T3-85	bC	78.15	265
LM01	pbC	79.10	175
LM02	pbC	79.05	50
LM04	UbC	81.63	0
LM05	UbC	82.98	-142
LM06	UbC	82.93	-285
LM07	UbC	81.97	-428
LM08	UbC	81.21	-571
LM09	UbC	82.02	-714
LM10	UbC	83.60	-857
CM04	UbC	86.77	-1000
PP36	UbC	83.25	-1750
PP35	UbC	82.78	-2000

Table 5. Microprobe data for figure 10, including rock type, mol percent magnesium, and height with respect to the Ultramafic - Banded Series contact.

Sample #	SiO2	Al2O3	TiO2	FeO	MnO	CaO	MgO	K2O	Na2O	P2O5	LOI	Total
mm-0	54.74	4.66	0.130	8.85	0.189	4.10	27.59	0.05	0.38	0.000	NA	100.69
mm-100	55.03	5.37	0.124	8.45	0.182	4.29	27.30	0.05	0.43	0.000	NA	101.23
mm-250	55.16	4.17	0.167	8.88	0.194	4.34	27.39	0.05	0.46	0.000	NA	100.81
mm-50	55.13	3.54	0.192	9.55	1.199	3.64	28.13	0.05	0.41	0.000	NA	100.84
mm-510	54.79	4.67	0.191	9.44	0.203	4.99	26.47	0.05	0.36	0.000	NA	101.16
mm-588	53.92	5.84	0.193	10.29	0.206	4.72	24.84	0.05	0.46	0.002	NA	100.52
mm-C	53.8	5.18	0.16	10.1	0.02	4.21	26.0	0.05	0.35	< 0.05	0.72	100.59
mm-F	53.3	5.13	0.22	11.8	0.21	4.88	24.2	0.04	0.32	< 0.05	0.66	100.76
WF-BC	54.3	2.88	0.13	10.6	0.21	3.20	28.1	0.02	<0.15	<0.05	0.45	99.89
cc-1	47.5	19.6	0.10	5.05	0.09	11.5	10.9	0.25	0.80	<0.05	3.45	99.24
cc-2	50.7	11.2	1.02	12.2	0.13	7.85	11.2	0.10	0.52	<0.05	3.82	98.74
cc-3	52.3	5.97	0.21	10.5	0.27	6.06	19.7	0.02	<0.15	<0.05	4.39	99.42
cc-4	43.6	15.8	0.17	10.0	0.14	10.1	14.8	0.08	0.57	<0.05	3.93	99.19
cc-8	50.7	13.2	0.16	9.74	0.17	8.98	15.3	0.07	0.82	<0.05	0.98	100.12
cc-9	50.4	8.10	0.23	15.0	0.23	5.45	17.9	0.10	0.32	<0.05	2.44	100.17
cc-10	51.7	7.01	0.19	13.0	0.22	7.07	20.1	0.04	0.46	< 0.05	0.83	100.62
cc-10	46.0	26.1	0.08	4.62	0.07	13.0	6.59	0.13	1.51	<0.05	1.62	99.72
cc-11	51.9	7.33	0.19	11.8	0.19	6.85	19.8	0.04	0.46	<0.05	1.19	99.75
cc-12	52.0	7.04	0.21	12.5	0.23	6.87	20.3	0.07	0.53	< 0.05	1.06	100.81
cc-13	52.5	8.86	0.16	9.02	0.18	7.64	20.8	0.06	0.45	<0.05	0.48	100.15
cc-14	51.4	10.5	0.11	9.10	0.17	6.65	19.8	0.05	0.48	<0.05	1.29	99.55
cc-15	54.0	3.73	0.14	10.2	0.21	4.64	26.3	0.02	0.22	<0.05	0.27	99.73
cc-101	48.4	24.4	0.08	4.02	0.07	13.5	7.53	0.06	1.19	<0.05	0.70	99.95
cc-102	47.0	25.4	0.09	3.64	0.06	14.9	5.66	0.12	1.44	<0.05	1.18	99.49
cc-103	49.5	16.4	0.13	5.23	0.12	14.4	11.5	0.07	0.86	<0.05	1.10	99.31
cc-104	49.6	20.6	0.01	5.40	0.10	12.5	10.6	0.05	0.93	<0.05	0.22	100.01
cc-105	46.7	28.0	0.10	3.01	0.05	14.8	3.91	0.15	1.76	<0.05	1.32	99.80
cc-107	48.4	11.1	0.16	10.4	0.20	4.81	16.6	0.02	<0.15	<0.05	7.86	99.55
cc-108	48.3	4.85	0.22	16.9	0.21	4.81	19.2	0.02	<0.15	<0.05	4.87	99.38
cc-109	47.1	6.20	0.26	18.9	0.25	4.76	18.1	0.03	<0.15	<0.05	4.03	99.63
cc-110	47.4	20.9	0.08	5.68	0.10	11.1	11.6	0.10	0.91	<0.05	1.74	99.61
cc-112	51.1	6.60	0.20	14.1	0.23	5.88	20.5	0.05	0.42	<0.05	0.58	99.66
cc-113	46.7	21.3	0.11	7.18	0.17	9.57	7.83	0.02	1.70	<0.05	4.90	99.48
cc-114	46.9	23.0	0.11	5.84	0.09	12.0	8.89	0.09	1.16	<0.05	1.85	99.93
cc-115	51.4	10.6	0.13	9.75	0.17	6.71	19.8	0.04	0.55	<0.05	0.40	99.55
cc-116	45.9	20.5	0.09	6.37	0.10	11.1	11.1	0.09	1.09	<0.05	3.16	99.50
cc-117	53.6	4.78	0.14	9.99	0.19	4.09	26.0	0.05	0.30	<0.05	0.84	99.98
cc-118	53.9	2.16	0.19	10.3	0.19	2.67	28.1	0.05	< 0.15	<0.05	1.74	99.30
cc-119	52.3	10.8	0.51	11.4	0.13	8.33	11.4	0.14	0.61	<0.05	3.11	98.73
cc-120	53.3	5.57	0.17	10.1	0.20	5.50	24.2	0.04	0.33	<0.05	0.61	100.02
cc-121	52.0	6.12	0.17	11.9	0.21	5.15	22.8	0.03	0.31	<0.05	0.79	99.48
cc-122	40.1	6.14	0.09	12.8	0.13	3.05	29.3	0.02	<0.15	<0.05	8.05	99.68
cc-123	52.2	7.98	0.16	11.6	0.22	5.27	21.3	0.08	0.45	<0.05	0.85	100.11
cc-124	49.5	9.89	0.19	11.3	0.20	5.26	17.8	0.02	<0.15	<0.05	4.85	99.01
cc-126	46.9	21.5	0.11	4.77	0.12	9.62	9.60	0.98	2.21	<0.05	3.57	99.38
cc-127	49.9	8.85	0.17	11.9	0.20	5.82	18.8	0.05	0.46	<0.05	3.05	99.20
cc-128	49.5	10.2	0.19	10.9	0.24	5.38	17.6	0.05	0.29	<0.05	5.16	99.51
cc-130	51.3	6.74	0.19	14.1	0.23	5.41	20.8	0.05	0.42	<0.05	0.49	99.73
cc-131	46.1	25.0	0.10	5.69	0.09	9.14	5.19	1.29	1.88	<0.05	4.07	98.55
cc-200	52.4	4.60	0.21	17.5	0.28	2.96	22.4	0.07	0.19	<0.05	0.10	100.71
cc-AP	51.1	7.85	0.18	12.9	0.21	5.63	19.8	0.06	0.46	<0.05	1.29	99.48
cc-T1-5f	51.5	11.3	0.13	8.91	0.16	7.45	18.9	0.07	0.62	<0.05	0.91	99.95
cc-T1-20f	52.6	7.91	0.12	10.1	0.19	5.86	22.3	0.04	0.41	<0.05	0.56	100.09
cc-T1-25f	52.2	7.60	0.13	10.7	0.19	6.14	21.9	0.04	0.42	<0.05	0.39	99.71
cc-T1-10	51.1	15.0	0.16	8.48	0.15	9.23	14.8	0.06	0.90	<0.05	0.33	100.21
cc-T1-22	49.1	19.2	0.11	6.64	0.12	11.4	11.2	0.07	0.93	<0.05	0.82	99.59
cc-T1-25	52.1	9.76	0.14	9.33	0.17	6.41	20.7	0.05	0.50	<0.05	0.64	99.80
cc-T1-25	52.0	8.77	0.17	11.8	0.21	0.21	19.8	0.04	0.05	<0.05	0.35	93.40
cc-T1-35	51.5	9.33	0.17	13.1	0.22	5.75	19.0	0.06	0.49	<0.05	0.30	99.92
cc-T1-45	49.3	18.8	0.10	5.85	0.11	12.7	10.9	0.06	0.96	<0.05	0.93	99.71
cc-T1-55	48.6	20.2	0.08	5.28	0.10	0.10	10.9	0.05	0.94	<0.05	1.60	87.85
cc-T1-65	51.3	11.2	0.15	9.96	0.18	8.69	17.3	0.05	0.60	<0.05	0.43	99.86
cc-T1-80	52.8	5.92	0.17	13.0	0.23	4.94	22.7	0.04	0.29	<0.05	0.15	100.24
cc-T1-90	52.3	5.87	0.17	12.4	0.19	4.38	22.7	0.04	0.27	<0.05	1.48	99.80

Table 6. Whole rock analyses (XRF) of Coors area and Mouat Mine road  
Samples given in weight percent. (contin. on next page)

Sample #	SiO2	Al2O3	TiO2	FeO	MnO	CaO	MgO	K2O	Na2O	P2O5	LOI	Total
cc-T1-95	51.1	8.09	0.17	12.3	0.20	0.20	19.9	0.05	0.39	<0.05	2.04	94.44
cc-T1-105	49.0	21.4	0.08	4.79	0.09	13.0	9.80	0.05	0.97	<0.05	0.63	99.81
cc-T1-110	49.5	20.1	0.08	5.41	0.11	11.3	11.7	0.05	0.89	<0.05	0.59	99.73
cc-T1-130	48.3	21.7	0.07	4.65	0.09	13.1	9.33	0.05	0.99	<0.05	1.06	99.34
cc-T1-135	51.2	11.0	0.16	12.1	0.20	6.35	18.2	0.06	0.57	<0.05	0.24	100.08
cc-T2-5	52.1	3.74	0.25	17.0	0.27	2.89	22.8	0.05	0.20	<0.05	0.80	100.10
cc-T2-10	50.1	16.1	0.10	6.88	0.13	9.64	14.8	0.06	0.74	<0.05	1.44	99.99
cc-T2-15	52.3	1.69	0.29	18.6	0.29	1.77	23.8	0.04	<0.15	<0.05	1.21	99.99
cc-T2-20	50.0	11.4	0.21	12.8	0.21	6.42	16.6	0.09	0.58	<0.05	1.26	99.57
cc-T2-23	51.6	6.47	0.20	14.7	0.24	4.18	21.1	0.06	0.32	<0.05	1.00	99.87
cc-T2-25	47.4	23.7	0.07	3.79	0.09	13.1	7.29	0.23	1.27	<0.05	2.40	99.34
cc-T2-33	52.5	4.99	0.20	15.3	0.25	3.89	22.2	0.04	0.31	<0.05	0.50	100.18
cc-T2-35	51.1	12.7	0.11	7.60	0.15	9.56	17.2	0.05	0.57	<0.05	0.67	99.71
cc-T2-55	47.4	21.3	0.12	4.67	0.11	12.4	9.13	0.20	1.19	<0.05	2.53	99.05
cc-T2-60	49.1	18.7	0.07	5.55	0.11	11.8	11.7	0.08	0.90	<0.05	1.40	99.41
cc-T2-65	48.8	22.0	0.09	4.46	0.09	13.0	9.36	0.08	1.03	<0.05	0.79	99.70
cc-T2-75	49.5	19.1	0.09	5.63	0.11	11.4	12.1	0.09	0.89	<0.05	0.80	99.71
cc-T3-10	50.5	9.58	0.22	14.1	0.24	5.66	17.8	0.12	0.55	<0.05	0.99	99.76
cc-T3-15	53.0	1.44	0.33	19.4	0.30	1.60	23.9	0.04	<0.15	<0.05	1.06	101.07
cc-T3-20	52.0	1.94	0.32	19.1	0.29	1.74	23.8	0.04	<0.15	<0.05	1.09	100.32
cc-T3-25	53.6	3.93	0.12	10.4	0.20	3.94	26.7	0.10	0.15	<0.05	0.79	99.93
cc-T3-30a	51.3	5.87	0.26	16.6	0.27	3.75	20.7	0.10	0.32	<0.05	1.03	100.20
cc-T3-30b	51.1	6.17	0.27	16.4	0.27	3.83	20.4	0.12	0.36	<0.05	0.95	99.87
cc-T3-35	52.1	2.73	0.30	18.2	0.29	2.21	23.0	0.06	<0.15	<0.05	0.82	99.71
cc-T3-40	51.2	5.02	0.26	16.9	0.28	3.37	21.2	0.11	0.27	<0.05	1.24	99.85
cc-T3-45	50.7	6.81	0.27	15.9	0.26	4.11	19.6	0.11	0.39	<0.05	1.53	99.68
cc-T3-5	49.7	19.1	0.09	5.88	0.11	0.11	12.1	0.05	0.87	<0.05	0.57	88.58
cc-T3-60	52.4	6.40	0.24	14.2	0.25	0.25	20.3	0.05	0.44	<0.05	0.07	94.60
cc-T3-70	50.1	9.61	0.12	10.6	0.18	0.18	19.3	0.05	0.45	<0.05	1.89	92.48
cc-T3-70a	49.5	7.13	0.14	12.7	0.20	0.20	20.0	0.05	0.34	<0.05	2.54	92.80
cc-T3-75	52.3	7.65	0.13	11.3	0.20	0.20	22.1	0.04	0.37	<0.05	0.54	94.83
cc-T3-80	52.5	5.97	0.15	12.4	0.22	4.82	22.8	0.04	0.32	<0.05	0.71	99.93
cc-T3-85	52.7	4.61	0.16	13.2	0.24	3.75	24.5	0.04	0.21	<0.05	0.45	99.86
cc-T3-90	51.9	7.70	0.13	11.8	0.20	5.41	21.6	0.04	0.39	<0.05	0.73	99.90
8-414-25	47.4	3.57	0.09	10.1	0.13	3.08	28.2	0.04	<0.15	<0.05	6.41	99.02
8-425-35	46.7	2.51	0.08	11.3	0.19	2.77	30.7	0.03	<0.15	<0.05	5.38	99.66
8-489-99	50.8	2.64	0.23	12.4	0.21	3.56	27.0	0.04	<0.15	<0.05	0.75	97.63
8-555-65	53.6	1.99	0.15	10.6	0.20	3.99	27.8	0.05	<0.15	<0.05	0.99	99.37
8-565-74	52.2	3.56	0.12	10.1	0.19	3.92	27.5	0.15	<0.15	<0.05	2.09	99.83
8-573-04	52.8	2.74	0.12	10.8	0.20	3.07	28.7	0.09	<0.15	<0.05	1.47	99.99
8-574-84	50.5	3.54	0.11	10.5	0.19	3.64	28.2	0.12	<0.15	<0.05	3.19	99.99
8-584-93	53.4	1.73	0.15	11.2	0.20	2.82	28.5	0.03	<0.15	<0.05	1.57	99.60
9-229-38	51.0	13.5	0.10	8.11	0.15	9.02	16.9	0.03	0.61	<0.05	0.53	99.95
9-233-48	51.5	11.4	0.11	8.90	0.16	7.89	18.9	0.04	0.52	<0.05	0.76	100.18
9-24-32	50.0	16.8	0.15	7.28	0.13	11.5	12.2	0.09	0.98	<0.05	0.60	99.73
9-32-41	51.4	11.7	0.17	9.92	0.18	8.21	17.0	0.08	0.73	<0.05	0.63	100.02
9-334-43	52.3	7.51	0.20	11.1	0.20	5.93	21.0	0.10	0.45	<0.05	0.70	99.49
9-562-72	52.3	5.55	0.22	14.4	0.25	5.37	21.6	0.05	0.31	<0.05	0.31	100.36
9-601-10	52.1	5.14	0.22	16.3	0.27	3.64	22.1	0.06	0.24	<0.05	0.16	100.23
9-62-71	49.3	19.6	0.09	5.71	0.11	11.9	11.3	0.05	0.92	<0.05	1.04	100.02
9-638-47	51.9	9.20	0.18	12.0	0.22	6.36	19.3	0.08	0.54	<0.05	0.46	100.24
9-647-56	52.2	6.95	0.19	13.1	0.23	5.79	21.0	0.05	0.41	<0.05	0.35	100.27
9-71-80	49.5	19.5	0.09	5.81	0.11	11.5	11.6	0.06	0.92	<0.05	0.81	99.90
11-172-82	52.0	4.58	0.20	14.9	0.25	3.48	23.0	0.07	0.24	<0.05	1.31	100.03
11-184-92	52.5	4.44	0.21	14.6	0.25	3.81	23.2	0.06	0.22	<0.05	1.04	100.33
11-192-01	52.4	2.33	0.24	15.7	0.26	4.17	24.0	0.04	<0.15	<0.05	0.98	100.12
11-249-58	51.7	6.29	0.21	13.1	0.22	5.38	20.9	0.08	0.48	<0.05	1.56	99.92
11-277-87	52.4	5.78	0.21	13.9	0.24	4.90	21.9	0.06	0.40	<0.05	0.60	100.39
11-314-24	49.1	20.6	0.08	5.23	0.10	12.1	10.6	0.06	0.95	<0.05	0.80	99.62
11-324-332	48.9	21.2	0.09	4.83	0.09	12.8	9.97	0.07	0.99	<0.05	1.07	100.01
11-341-50	48.6	22.6	0.09	4.43	0.08	12.7	8.96	0.14	1.05	<0.05	1.26	99.91
11-359-72	46.1	25.7	0.06	3.24	0.06	13.9	5.63	0.19	1.34	<0.05	3.39	99.61
11-372-82	46.4	26.7	0.06	2.75	0.05	14.2	4.95	0.18	1.32	<0.05	3.08	99.69

Continued from previous page

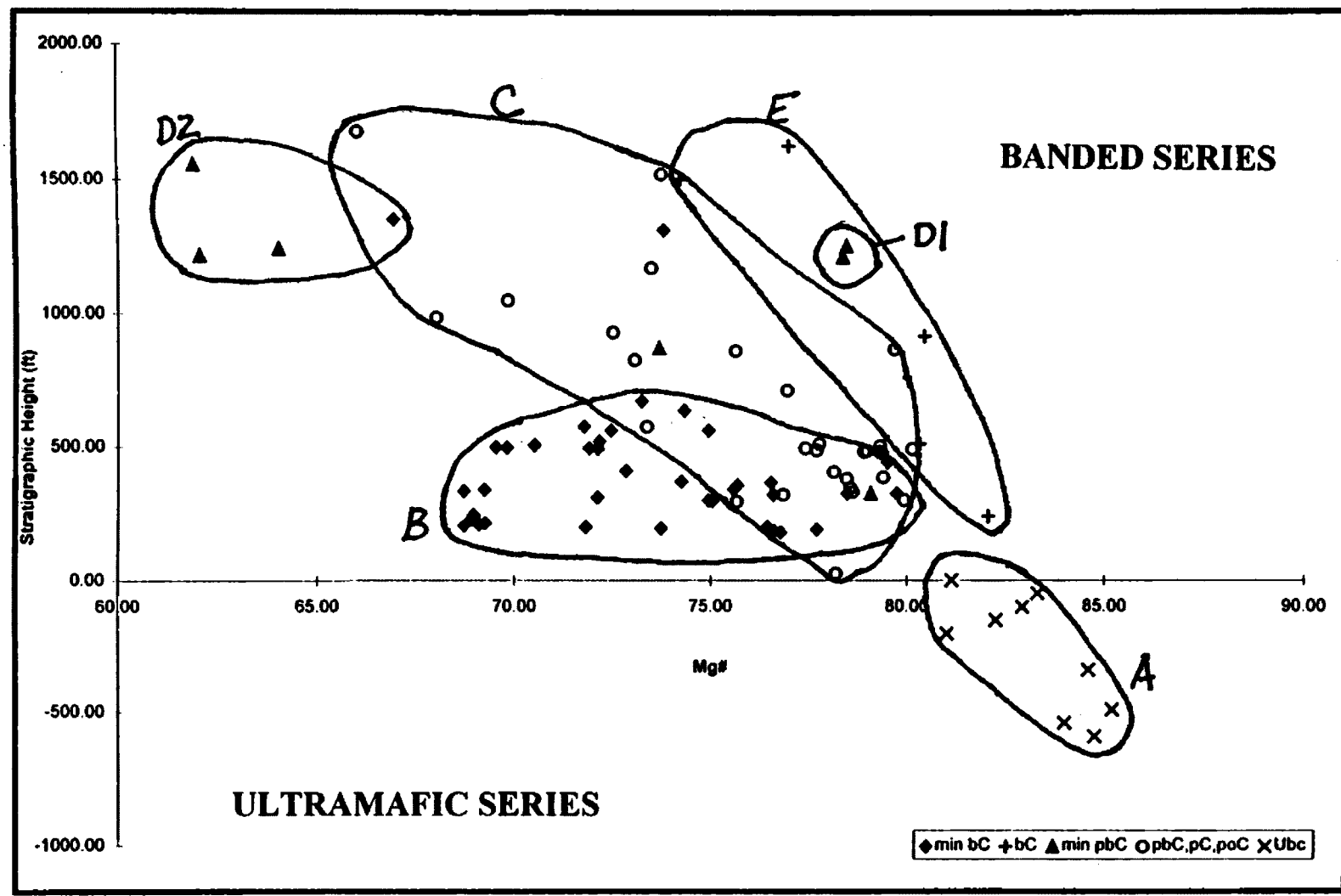


Figure 11. Plot of stratigraphic height versus magnesium number (mol percent Mg) of whole rocks using the Banded Series - Ultramafic Series contact as the datum. Data is based on Coors area whole rock analyses (XRF).

Sample #	Rock Type	mol% Mg	Height	Sample #	Rock Type	mol% Mg	Height	Sample #	Rock Type	mol% Mg	Height
mm-0	UbC	84.75	-588	cc-116	pC	75.65	860	cc-T1-130	pbC	78.15	405
mm-50	UbC	84.00	-538	cc-117	UbC	82.27	-150	cc-T1-135	pbC	72.83	410
mm-100	UbC	85.20	-488	cc-118	UbC	82.94	-100	cc-T2-5	bC	70.51	505
mm-250	UbC	84.61	-338	cc-119	pbC	64.06	1240	cc-T2-10	pbC	79.31	501
mm-510	UbC	83.33	-50	cc-120	UbC	81.03	-200	cc-T2-15	bC	69.52	499
mm-588	UbC	81.14	0	cc-121	UbC	77.35	-75	cc-T2-20	bC	69.80	497
mm-C	UbC	82.11	-10	cc-122	bC	80.32	510	cc-T2-23	bC	71.90	495
mm-F	UbC	78.52	-20	cc-123	bC	76.60	320	cc-T2-25	pbaC	77.42	494
cc-1	pbC	79.37	475	cc-124	pbC	73.74	1520	cc-T2-33	bC	72.12	492
cc-2	pbC	62.07	1215	cc-126	UbC	78.20	25	cc-T2-35	bC	80.13	491
cc-3	bC	76.98	1605	cc-127	pbC	73.79	1310	cc-T2-55	pbC	77.70	486
cc-4	poC	72.51	930	cc-128	pC	74.21	1500	cc-T2-60	bC	78.98	484
cc-8	poC	73.68	870	cc-130	bC	72.45	560	cc-T2-65	pbC	78.91	482
cc-9	pbC	68.02	985	cc-131	pbC	61.92	1555	cc-T2-75	pbC	79.30	480
cc-10	bC	73.38	575	cc-AP	bC	73.23	670	cc-T3-5	pbC	78.58	345
cc-10	pbC	71.77	575	cc-T1-5f	pbC	79.08	325	cc-T3-10	bpC	69.23	340
cc-11	bpC	74.94	560	cc-T1-20f	bC	79.74	325	cc-T3-15	bC	68.71	335
cc-12	bC	74.32	635	cc-T1-25f	bC	78.49	325	cc-T3-20	bC	68.95	330
cc-13	bC	80.43	915	cc-T1-10	pbC	75.67	295	cc-T3-25	bC	82.07	325
cc-14	pbC	79.50	440	cc-T1-22	pbC	75.04	297	cc-T3-30a	bC	68.97	315
cc-101	pC	76.95	710	cc-T1-25a	bC	79.82	300	cc-T3-30b	bC	68.92	315
cc-102	pbC	73.49	1170	cc-T1-25b	bC	74.94	300	cc-T3-35	bC	69.25	300
cc-103	pbC	79.67	865	cc-T1-35	bpC	72.11	310	cc-T3-40	bC	69.10	295
cc-104	pC	77.77	510	cc-T1-45	pbC	76.86	320	cc-T3-45	bC	68.72	290
cc-105	pbC	69.84	1050	cc-T1-55	pbC	78.63	330	cc-T3-60	bC	71.82	285
cc-108	bC	66.94	1350	cc-T1-65	pbC	75.59	340	cc-T3-70	bC	76.44	280
cc-110	pbC	78.45	1250	cc-T1-80	bC	75.68	355	cc-T3-70a	bC	73.73	280
cc-112	bC	72.16	520	cc-T1-90	bC	76.54	365	cc-T3-75	bC	77.71	275
cc-113	pC	66.03	1680	cc-T1-95	bC	74.25	370	cc-T3-80	bC	76.62	270
cc-114	poC	73.07	825	cc-T1-105	pbC	78.48	380	cc-T3-85	bC	76.79	265
cc-115	pbC	78.35	1210	cc-T1-110	pbC	79.40	385	cc-T3-90	bC	76.54	260

Table 7. Data for figure 11, including rock type, mol percent magnesium, and height in feet.

Mg number's. The JM Reef mineralized samples (D1 on Fig. 11) and the unmineralized samples (groups C and E in Fig. 11) have the highest Mg numbers.

### **PGE Sulfides**

The trench samples were assayed by Stillwater PGM labs for nickel, copper, platinum, and palladium (Table 8). Values range from <50 to 1550 ppm nickel, <20 to 1650 ppm copper, <50 to 14600 ppb platinum, and <20 to 34000 ppb palladium. As seen in table 8, the ratio of Pd to Pt averages 1.77 for trench samples. Coors and Mouat Mine samples were also analyzed for PGE's Cu and Ni.. These analyses are listed in table 9. The average Pd to Pt ratio in these samples is 1.2. The JM reef has an average Pd:Pt ratio of 3.5 to 1. Figures 12a and 12b show a positive correlation between Pd and Pt. Note that samples 102, 110, 115 have ratios above 3.0. These three samples are from the JM reef. Positive correlations also exist between copper and nickel versus palladium and copper and nickel versus platinum in both sets of analyses (Figs. 13 and 14).

	Cu	Ni	Pt	Pd	Pd/Pt	type	% plbg	% eule	sl size (cm)	peg
<b>C636T-1</b>										
150	264	125	130	1.04	pbC	35-45			.3-.5	
232	272	75	115	1.53	pbC	50			0.3	
257	285	85	85	1.31	pbC	30-60	tr-1		.3-.5	
164	225	100	95	0.95	pbC	60-70	tr-5		.3-.5	
142	230	50	85	1.30	pbC	60-70	tr-5		.3-.5	
72	320	<50	50		pbC	50	tr		.5-1.5	p
80	450	<50	85		bC	10-30	tr-1		.3-.5	
372	500	425	380	0.89	bC	10-30	tr-1		.3-.5	
372	490	525	555	1.06	bC	10-30	tr-1		.3-.5	
435	580	425	1,250	2.94	bC	10-30	tr-1		.3-.5	
600	550	700	515	0.74	bC	10-15	1		0.3	
289	595	575	455	0.79	bC	10-15	1		.5-.7	
680	1,075	450	410	0.91	bC	<5	1		0.5	
370	480	850	550	0.85	bC	10-15	1		0.5	
740	870	900	800	0.87	bC	10-20	tr-5		.5-1.5	p
920	1,250	800	950	1.19	bC	10-20	3-5		.5-1.5	p
420	475	550	430	0.78	bC	10-20	3-5		.5-1.5	p
910	1,085	925	800	0.86	bC	10	1-3		.5-1.5	p
530	600	775	750	0.97	bC	10-20	1-5		.5-1.5	p
255	380	150	130	0.87	bC	10-20	1-5		.5-1.0	p
318	450	75	70	0.93	bC	10-20	1-5		.5-1.0	p
405	570	175	130	0.74	pbC	50-60			.5-1.0	p
36	103	<50	20		pbC	50-60			.5-1.0	p
17	65	<50	20		pbC	50-60			0.5	
14	70	<50	25		pbC	50-60			0.5	
14	54	<50	25		pbC	50-60			0.5	
16	60	50	25	0.50	pbC	50-60			0.5	
178	390	300	245	0.92	bC	20-35	tr-2		.1-.5	
190	340	200	245	1.23	bC	20-35	tr-2		.1-.5	
192	330	200	220	1.10	bC	20-35	tr-2		.1-.5	
166	295	200	170	0.85	bC	20-35	tr-2		.1-.5	
380	430	500	300	0.80	bC	20-35	tr-2		.1-.5	
352	485	500	325	0.85	bC	20-50	1-2		.3-.4	
49	98	100	60	0.80	pbC	60-70			.3-.4	
18	52	50	30	0.80	pbC	60-70			.3-.4	
12	50	50	25	0.50	pbC	60-70			.3-.4	
<b>C602T-2</b>										
288	325	650	1,700	2.62	bC	10	tr		<.3	peg
118	168	150	188	1.20	pbC	50-60	0-5		0.4	
324	300	1,400	3,700	2.64	bC	10	tr-5			peg
385	380	675	1,800	2.67	bC	10	tr-5			peg
500	425	325	585	1.83	bC	10	tr-5		<.3	peg
53	200	<50	45		pbC	60				
22	212	<50	70		pbC	60	0			
98	212	50	80	1.20	pbC	60				
224	385	350	1,000	2.86	bC	20	tr-5		.5-1	peg
590	520	2,700	8,000	3.33	bC	20	tr-5		.5-1	peg
435	440	800	2,500	3.13	bC	20	tr		<.2	peg
292	324	300	425	1.42	bC	20	tr		<.2	
164	220	100	120	1.20	bC	<5	tr		.2-.7	
142	200	125	100	0.80	bC	<5	tr		.8-.7	
144	212	125	90	0.72	bC	<5	tr		.2-.7	
58	164	75	80	1.07	pbC	60			.3-.5	
16	54	75	55	0.73	pbC	60			.3-.5	
20	54	50	75	1.50	pbC	60			.3-.5	
<b>C602T-1</b>										
560	700	1,800	2,750	1.72	bC	20	tr		<1.5	peg
158	190	100	145	1.45	bC	20	tr-1		.3-.6	
68	138	50	85	1.70	pbC	40	tr		.1-1.0	peg
173	232	75	225	3.00	pbC	40	tr		.1-1.0	peg
130	188	50	75	1.50	pbC	40	tr		.1-1.0	peg
128	242	100	395	3.95	pbC	40	tr		.1-1.0	peg
233	405	600	2,200	3.67	bC	20	tr-5		1-1.5	peg
875	490	3,800	9,200	2.56	bC	20	tr-5		1-1.5	peg
460	505	2,250	6,400	2.84	bC	20	tr-5			
228	364	150	600	4.00	bC	20	tr-5			
60	110	50	80	1.60	pbC	40-50			.3-1	peg
156	180	50	80	1.60	pbC	40-50			.3-2	peg
285	380	400	1,200	3.00	pbC	40-50			.3-3	peg
280	338	400	1,400	3.50	pbC	40-50			.3-4	peg
460	375	1,050	4,000	3.81	bC	20-30	tr-1		1-1.5	peg
344	350	550	1,700	3.09	bC	20-30	tr-1		1-1.6	peg
392	400	325	1,700	5.23	bC	20-30	tr-1		1-1.7	peg
805	480	8,200	11,000	1.77	bC	20-30	tr-1		1-1.8	peg
855	820	8,800	13,000	1.91	bC	20-30	tr-1		1-1.9	peg
1,850	1,450	14,800	34,000	2.33	bC	5	tr-5		1-1.5	peg
450	430	1,450	5,500	3.79	bC	20	tr		1	peg
440	385	1,450	4,700	3.24	bC	20	tr		1-2	peg
67	162	50	105	2.10	pbC	50-60			.3-.5	
50	138	50	85	1.30	pbC	50-60				
72	118	300	620	2.07	pbC	50-60				
28	60	50	40	0.80	pbC	50-60				
28	68	50	25	0.50	pbC	50-60				
252	338	200	280	1.40	bC	20	tr		1	peg
292	385	425	1,000	2.35	bC	20	tr		1	peg
<b>C602T-3</b>										
38	65	<50	20		pbC	80				
32	70	<50	25		pbC	80			.3-.4	
180	390	<50	55		bC	5-25	0-tr			
249	570	100	210	2.10	bC	5-15	tr-5		<.1	peg
242	445	150	330	2.20	bC	10	1		<.1	peg
338	750	200	435	2.18	bC	<1			<.1	peg
144	340	50	80	1.60	bC	10-20			.5-2	peg
300	440	200	275	1.38	bC	10-20	0-tr		<.3	peg
460	575	325	400	1.23	bC	5	0-tr			
200	380	250	800	3.20	bC	5	0-tr			
352	510	2,800	6,900	2.46	bC	5	0-tr			
1,280	1,150	10,000	26,000	2.60	bC	5	0-tr		1	peg
1,350	1,550	5,550	22,000	3.98	bC	5	5-10			
850	875	3,050	5,500	1.80	bC	5	tr-2		<.2	peg
460	495	200	240	1.20	bC	10-20	tr-2		.2-1.2	peg
580	685	325	350	1.08	bC	10-20	tr-2		.2-1.2	peg
640	780	350	420	1.20	bC	10-20	tr-2		0.5	
388	400	350	620	1.77	bC	10-20	tr-2		.2-1.2	peg
Pd/Pt Avg = 1.77										

Table 8. Assay data including PGE analyses from trenches T1,T2, T3, and T635 from the Coors area. Data is expressed in ppm for copper and nickel and ppb for platinum and palladium. Assay data were provided by the Stillwater Mining Company

sample#	Cu (ppm)	Ni (ppm)	Pt (ppb)	Pd (ppb)	Rh (ppb)	Ru (ppb)	Ir (ppb)	Pt/Pd	Pd/Pt
nm-C	28	907	6.5	5.7	3.2	<1	<1	1.1	0.9
nm-F	47	907	29.0	11.0	6.9	1.0	<1	2.6	0.4
WF-BC	22	708	3.4	6.4	<0.5	<0.5	<0.5	0.5	1.9
cc-1	14	243	17.0	14.0	2.5	<0.5	<0.5	1.2	0.8
cc-2	168	488	500.0	440.0	14.0	10.0	4.0	1.1	0.9
cc-3	162	860	1.6	1.0	<0.5	<0.5	<0.5	1.6	0.6
cc-4	21	365	9.6	5.0	<0.5	<0.5	<0.5	1.9	0.5
cc-8	94	470	82.0	81.0	0.5	<0.5	<0.5	1.0	1.0
cc-9	86	488	13.0	11.0	<0.5	<0.5	<0.5	1.2	0.8
cc-10	25	385	850.0	1100.0	6.8	4.2	2.0	0.6	1.7
cc-10	686	360	7.2	5.4	<0.5	<0.5	<0.5	1.3	0.8
cc-11	170	640	590.0	590.0	2.9	2.1	1.0	1.0	1.0
cc-12	185	488	53.0	28.0	<1	<1	<1	1.9	0.5
cc-13	24	610	180.0	140.0	6.0	0.8	0.5	1.3	0.8
cc-14	68	880	570.0	560.0	6.6	0.9	0.5	1.0	1.0
cc-15	61	620	14.0	6.4	5.3	1.1	1.3	2.2	0.5
cc-101	13	140	35.0	19.0	3.2	<0.5	<0.5	1.8	0.5
cc-102	38	218	13.0	41.0	0.6	<0.5	<0.5	0.3	3.2
cc-103	24	260	22.0	11.0	2.0	<0.5	<0.5	2.0	0.5
cc-104	42	235	42.0	46.0	2.3	<0.5	<0.5	0.9	1.1
cc-105	30	175	7.5	5.8	0.5	<0.5	<0.5	1.3	0.8
cc-107	63	580	0.7	0.6	<0.5	<0.5	<0.5	1.2	0.9
cc-108	538	840	690.0	160.0	1.7	2.6	1.3	4.3	0.2
cc-109	388	670	390.0	260.0	1.8	1.6	0.9	1.5	0.7
cc-110	388	880	730.0	3100.0	28.0	7.6	3.1	0.2	4.2
cc-112	1088	2080	2400.0	2300.0	29.0	18.0	8.0	1.0	1.0
cc-113	82	280	2.0	2.0	<0.5	<0.5	<0.5	1.0	1.0
cc-114	32	385	1.9	2.2	0.5	<0.5	<0.5	0.9	1.2
cc-115	998	1788	6940.0	23300.0	170.0	67.0	26.0	0.3	3.4
cc-116	31	488	9.5	5.3	<0.5	<0.5	<0.5	1.8	0.6
cc-117	23	628	31.0	17.0	9.4	1.2	0.9	1.8	0.5
cc-118	33	670	17.0	13.0	7.8	1.4	1.1	1.3	0.8
cc-119	310	418	800.0	480.0	26.0	17.0	5.7	1.7	0.6
cc-120	41	880	17.0	7.9	5.3	0.6	<0.5	2.2	0.5
cc-121	67	475	210.0	18.0	19.0	1.4	1.2	11.7	0.1
cc-122	18	1788	290.0	210.0	28.0	4.9	2.2	1.4	0.7
cc-123	64	538	300.0	380.0	2.4	0.6	<0.5	0.8	1.3
cc-124	78	498	1.2	2.0	<0.5	<0.5	<0.5	0.6	1.7
cc-126	13	218	55.0	13.0	3.2	<0.5	<0.5	4.2	0.2
cc-127	388	840	390.0	370.0	4.0	2.6	1.1	1.1	0.9
cc-128	78	468	1.6	0.7	<0.5	<0.5	<0.5	2.3	0.4
cc-130	788	1688	3400.0	2800.0	31.0	22.0	9.3	1.2	0.8
cc-131	182	388	15.0	17.0	<0.5	<0.5	<0.5	0.9	1.1
cc-200	648	888	130.0	160.0	4.6	0.8	0.6	0.8	1.2
cc-AP	328	988	680.0	610.0	7.6	4.8	2.0	1.1	0.9
cc-T1-5f	268	638	980.0	2200.0	22.0	9.1	3.5	0.4	2.2
cc-T1-20f	182	728	350.0	650.0	4.8	1.8	0.7	0.5	1.9
cc-T1-25f	688	1388	3600.0	8500.0	80.0	30.0	12.0	0.4	2.4
cc-T1-10	118	488	38.0	64.0	<0.5	<0.5	<0.5	0.6	1.7
cc-T1-22	88	288	18.0	17.0	1.8	<0.5	<0.5	1.1	0.9
cc-T1-25	288	778	590.0	1100.0	12.0	4.8	1.8	0.5	1.9
cc-T1-25	188	618	73.0	160.0	1.2	<0.5	<0.5	0.5	2.2
cc-T1-35	298	688	97.0	140.0	1.4	0.9	<0.5	0.7	1.4
cc-T1-45	38	268	9.8	15.0	1.1	<0.5	<0.5	0.7	1.5
cc-T1-55	32	268	4.4	3.3	1.5	<0.5	<0.5	1.3	0.8
cc-T1-65	148	498	45.0	39.0	3.2	0.5	<0.5	1.2	0.9
cc-T1-80	278	618	150.0	230.0	3.6	1.0	<0.5	0.7	1.5
cc-T1-90	154	648	75.0	290.0	2.1	<0.5	<0.5	0.3	3.9
cc-T1-95	148	778	100.0	140.0	2.1	0.7	<0.5	0.7	1.4
cc-T1-105	28	228	29.0	54.0	2.1	<0.5	<0.5	0.5	1.9
cc-T1-110	23	288	22.0	14.0	2.7	<0.5	<0.5	1.6	0.8

sample#	Cu (ppm)	Ni (ppm)	Pt (ppb)	Pd (ppb)	Rh (ppb)	Ru (ppb)	Ir (ppb)	Pt/Pd	Pd/Pt
cc-T1-130	14	288	10.0	13.0	1.4	<0.5	<0.5	0.8	1.3
cc-T1-135	228	888	92.0	100.0	9.0	1.2	0.7	0.9	1.1
cc-T2-5	248	718	160.0	480.0	4.7	1.3	0.6	0.3	3.0
cc-T2-10	51	368	15.0	13.0	2.5	<0.5	<0.5	1.2	0.9
cc-T2-15	194	788	63.0	95.0	4.4	1.0	0.6	0.7	1.5
cc-T2-20	248	888	20.0	140.0	1.2	0.5	<0.5	0.1	7.0
cc-T2-23	316	698	13.0	31.0	0.7	<0.5	<0.5	0.4	2.4
cc-T2-25	18	174	18.0	21.0	2.8	<0.5	<0.5	0.9	1.2
cc-T2-33	225	728	82.0	200.0	1.4	0.7	<0.5	0.4	2.4
cc-T2-55	18	388	5.0	1.0	3.4	<0.5	<0.5	5.0	0.2
cc-T2-65	12	236	16.0	16.0	2.4	<0.5	<0.5	1.0	1.0
cc-T2-65	19	288	11.0	20.0	0.5	<0.5	<0.5	0.6	1.8
cc-T2-65	14	218	26.0	32.0	2.4	<0.5	<0.5	0.8	1.2
cc-T2-75	21	288	27.0	46.0	2.6	<0.5	<0.5	0.6	1.7
cc-T3-5	38	275	50.0	140.0	2.7	<0.5	<0.5	0.4	2.8
cc-T3-10	67	488	22.0	19.0	2.7	<0.5	<0.5	1.2	0.9
cc-T3-15	196	838	43.0	54.0	4.4	1.4	0.5	0.8	1.3
cc-T3-20	182	687	65.0	110.0	2.0	2.0	1.0	0.6	1.7
cc-T3-25	34	648	23.0	25.0	7.2	1.1	0.7	0.9	1.1
cc-T3-30a	54	638	20.0	36.0	1.0	0.6	<0.5	0.6	1.8
cc-T3-30b	92	638	20.0	32.0	0.5	0.6	<0.5	0.6	1.6
cc-T3-35	57	848	26.0	59.0	1.3	<0.5	<0.5	0.4	2.3
cc-T3-40	188	848	22.0	23.0	1.2	<0.5	<0.5	1.0	1.0
cc-T3-45	188	888	40.0	81.0	1.4	0.8	<0.5	0.5	2.0
cc-T3-60	118	628	52.0	69.0	0.7	<0.5	<0.5	0.6	1.3
cc-T3-70	1888	1488	5200.0	12000.0	100.0	40.0	14.0	0.4	2.3
cc-T3-70a	1888	2988	10000.0	35000.0	310.0	97.0	41.0	0.3	3.5
cc-T3-75	388	798	58.0	86.0	1.0	<0.5	<0.5	0.7	1.5
cc-T3-80	648	1188	110.0	150.0	2.7	1.0	<0.5	0.7	1.4
cc-T3-85	322	736	140.0	210.0	4.9	1.0	<1	0.7	1.5
cc-T3-90	348	1688	1100.0	2900.0	38.0	11.0	5.3	0.4	2.6
8-414-25	18	988	23.0	23.0	1.6	1.1	<0.5	1.0	1.0
8-425-35	38	1188	15.0	16.0	1.4	1.0	<0.5	0.9	1.1
8-489-99	298	1888	580.0	440.0	100.0	40.0	26.0	1.3	0.8
8-555-65	38	868	19.0	21.0	2.3	1.0	<0.5	0.9	1.1
8-565-74	21	678	22.0	37.0	3.4	1.8	0.7	0.6	1.7
8-573-04	25	718	8.5	11.0	1.8	1.7	<0.5	0.8	1.3
8-574-84	14	798	16.0	25.0	1.9	1.0	<0.5	0.6	1.6
8-584-83	41	888	12.0	22.0	1.5	1.1	<0.5	0.5	1.8
9-229-38	18	488	7.6	1.5	1.3	<0.5	<0.5	5.1	0.2
9-233-48	18	448	9.4	4.2	1.3	<0.5	<0.5	2.2	0.4
9-24-32	184	436	42.0	43.0	1.6	<0.5	<0.5	1.0	1.0
9-32-41	184	436	62.0	100.0	2.2	<0.5	<0.5	0.6	1.6
9-334-43	77	488	59.0	120.0	10.0	0.9	<0.5	0.5	2.0
9-562-72	298	788	180.0	110.0	4.1	0.7	<0.5	1.6	0.6
9-601-10	488	1888	230.0	260.0	11.0	1.3	0.5	0.9	1.1
9-62-71	12	248	22.0	17.0	2.2	<0.5	<0.5	1.3	0.8
9-638-47	218	688	11.0	16.0	<0.5	<0.5	<0.5	0.7	1.5
9-647-56	368	788	35.0	36.0	1.4	0.6	<0.5	1.0	1.0
9-71-80	18	248	28.0	20.0	2.5	<0.5	<0.5	1.4	0.7
11-172-82	648	1188	290.0	380.0	2.3	1.5	0.6	0.8	1.3
11-184-92	388	778	210.0	730.0	5.3	1.7	0.6	0.3	3.5
11-192-01	888	1888	580.0	1300.0	6.2	2.7	1.0	0.4	2.2
11-249-58	238	748	120.0	100.0	0.7	0.5	<0.5	1.2	0.8
11-277-87	124	648	30.0	13.0	<0.5	<0.5	<0.5	2.3	0.4
11-314-24	34	268	21.0	14.0	2.2	<0.5	<0.5	1.5	0.7
11-324-33	16	238	18.0	14.0	2.3	<0.5	<0.5	1.3	0.8
11-341-50	13	288	22.0	18.0	2.5	<0.5	<0.5	1.2	0.8
11-359-72	34	164	27.0	22.0	3.7	<0.5	<0.5	1.2	0.8
11-372-82	17	138	28.0	18.0	4.0	0.5	<0.5	1.6	0.6

Pd/Pt Avg = 1.2

Table 9. PGE, Cu and Ni analyses for Coors area and Mout Mine Road samples.



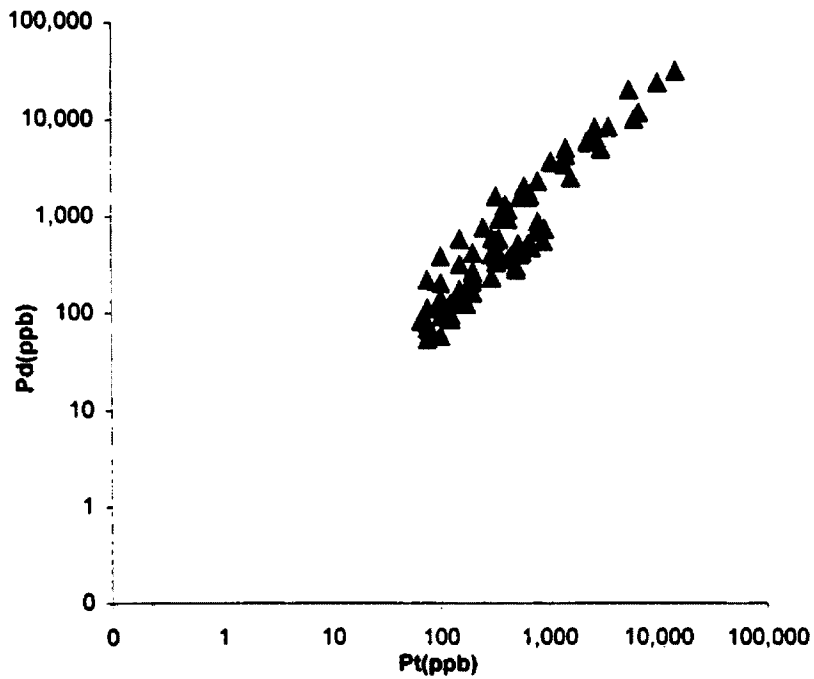


Figure 12a. Plot of palladium versus platinum for trench samples in the Coors area (Stillwater Mining Co. analyses).

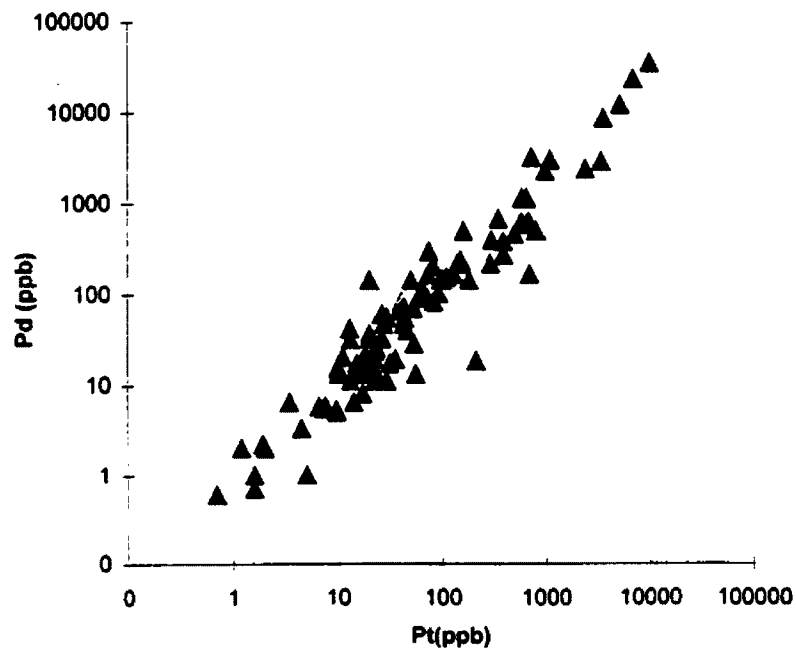


Figure 12b. Plot of palladium versus platinum for Coors area and Mouat mine road samples (USGS analyses this report).

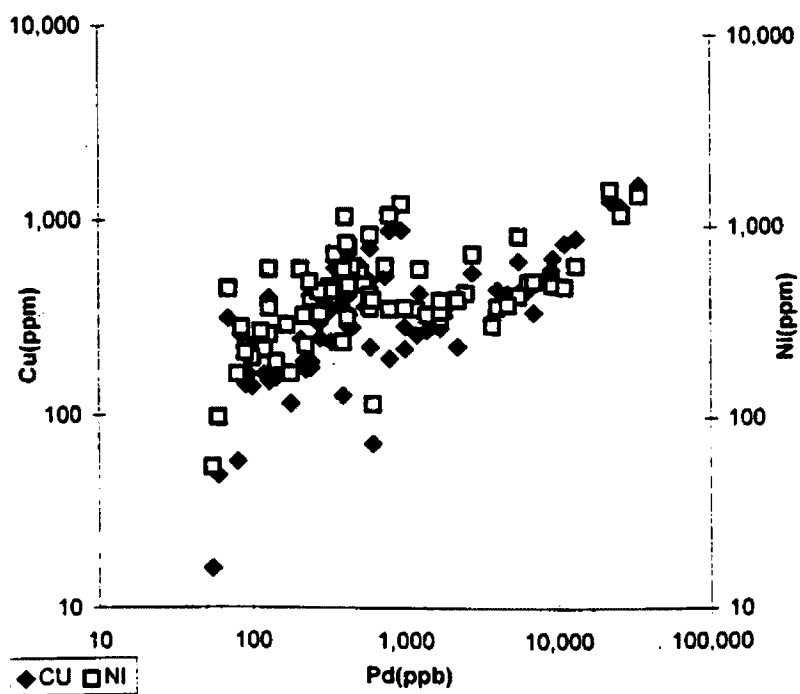


Figure 13a. Plot of copper and nickel versus palladium for trench samples in the Coors area (SMC).

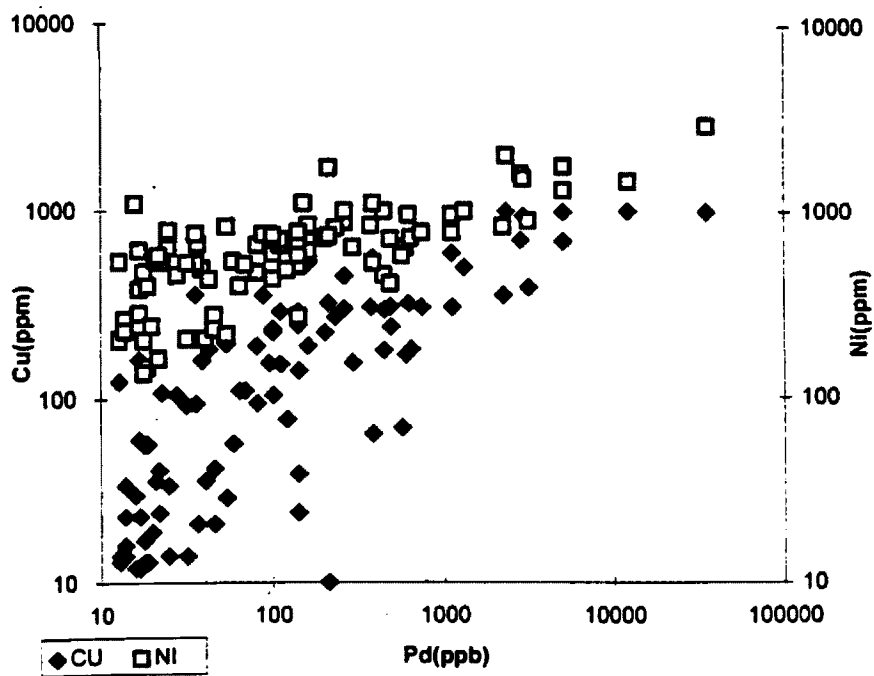


Figure 13b. Plot of copper and nickel versus palladium for Coors area and Mouat mine road samples.

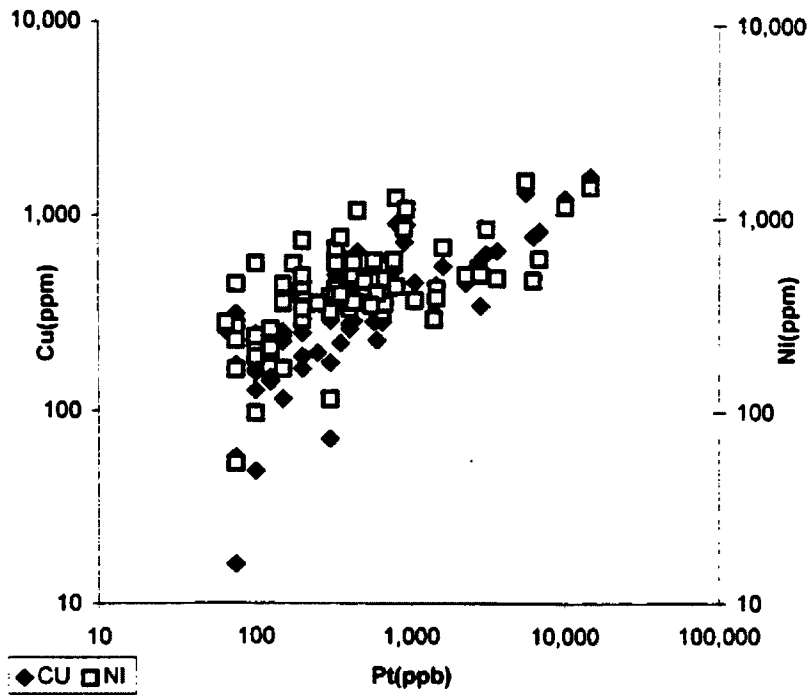


Figure 14a. Plot of copper and nickel versus platinum for trench samples in the Coors area (SMC).

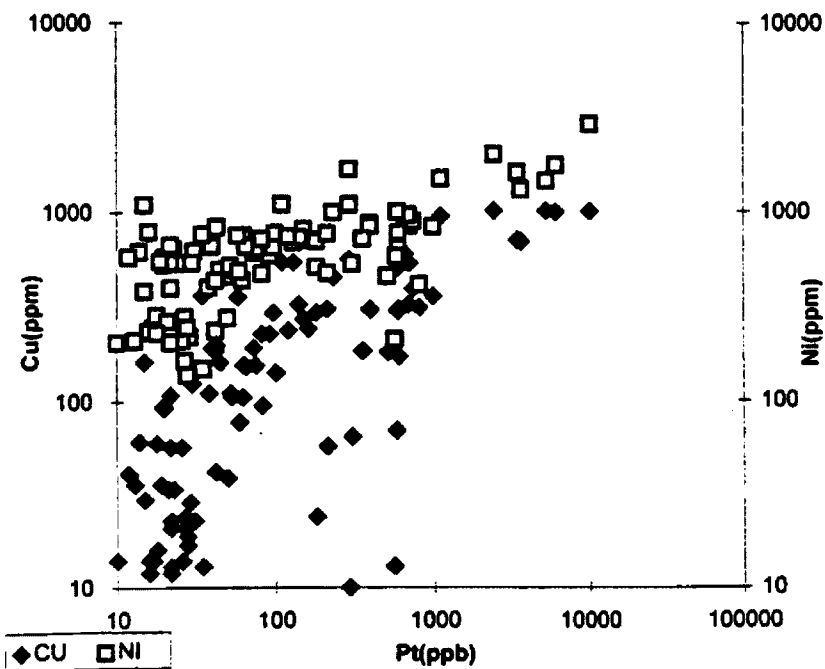


Figure 14b. Plot of copper and nickel versus platinum for trench samples in the Coors area (SMC).

## **INTERPRETATIONS**

### **JM REEF**

Numerous models have been proposed to explain the PGE-rich JM Reef. Because some of these ideas could relate to the Coors mineralization, several of the more accepted ones are discussed. Two general approaches exist, one involving a magmatic origin, the other involving a hydrothermal origin. Trace-element and isotopic studies of the parental magmas of the Stillwater Complex suggest that at least two different magmas were involved (Irvine et al., 1983, Lambert, 1982). The JM reef is thought to have formed as a result of mixing of these magmas; one of anorthositic lineage, A-type, and the other of ultramafic lineage, U-type (Todd et al., 1982; Irvine et al, 1983). Sulfur is thought to come from the anorthositic magma and PGE from the ultramafic magma. Other workers argue that the mixing was between the resident, sulfide-saturated magma with plagioclase on its liquidus and a less fractionated magma from the same parent (Naldrett et al., 1990; Campbell et al, 1983). Sulfide saturation in this latter theory is attained by crystallization of silicates to concentrate sulfur (Fig. 15, Naldrett et al, 1990).

Both theories state the need to have the sulfides exchange with a large amount of silicate magma. Campbell et al. (1983), derive the equation  $Y = XD(R+1)/(R=D)$  where R is the silicate- to sulfide-liquid mass ratio, Y is Pd/Pt, X is the initial concentration of Pd/Pt in the magma, and D is the Nernst distribution coefficient. This equation determines the PGE content of a magmatic sulfide liquid, and is illustrated in Figure 16. The R factor,

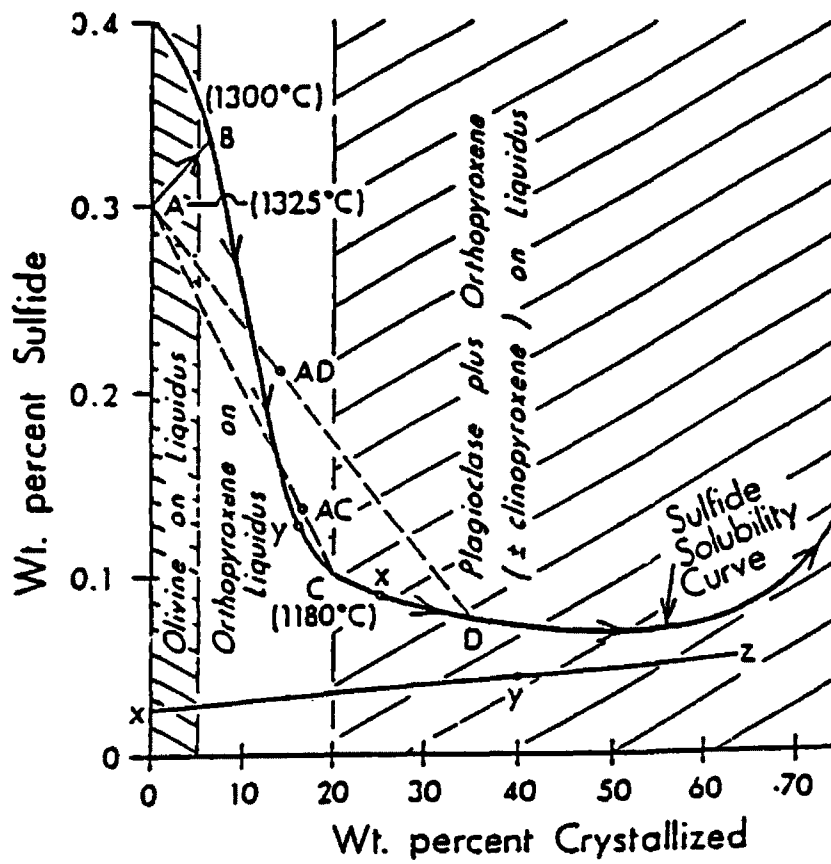


Figure 15. Schematic diagram illustrating the variation in the solubility of iron sulfide with the fractionation of a sample of chilled marginal material from the Bushveld Complex. (Naldrett, 1990)

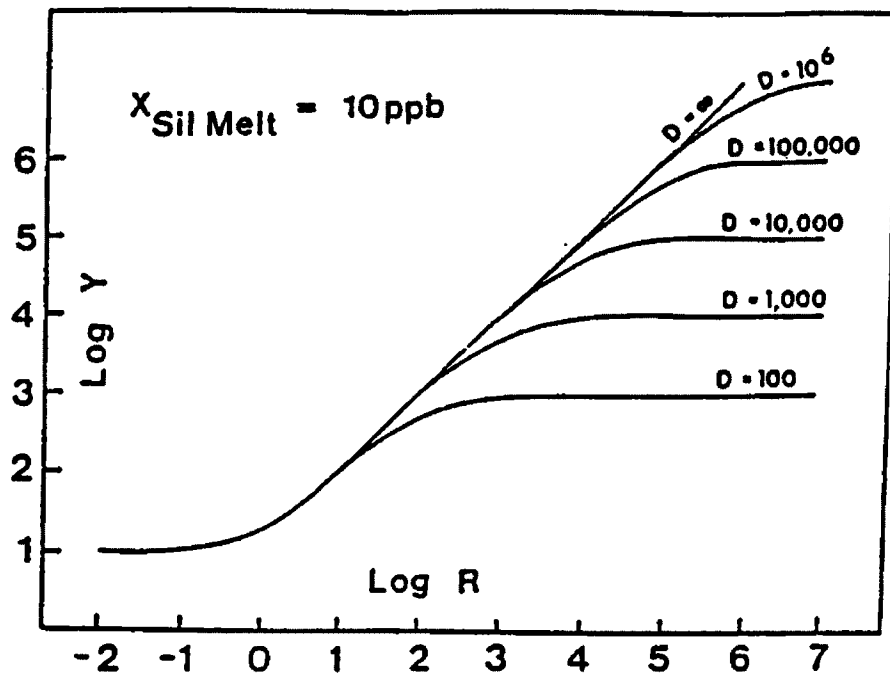


Figure 16. The effect of variations in the silicate:sulfide ratio ( $R$ ) on the precious metal content of a sulfide liquid for different values of  $D$ . The concentration of the precious metal in the silicate melt ( $X_1$ ) is assumed to be 10 p.p.b.. Note that if  $R$  is less than a tenth of  $D$ ,  $Y$  is virtually independent of  $D$ . (Naldrett, 1990)

the mass ratio of silicate to sulfide liquid, must be high in order for platinum to precipitate (Mathez et al., 1989; Naldrett et al., 1990). These authors suggest that turbulent mixing of the two magmas raised the R factor sufficient to allow the sulfides to scavenge PGE from the magma and precipitate (Naldrett et al., 1990).

Boudreau and McCallum, (1992), and Boudreau, (1988), present arguments for hydrothermal, in situ formation of the JM Reef. Boudreau (1988) suggested that a volatile-enriched melt was high in chlorine, or a chlorine-rich volatile fluid became locally concentrated, to produce the textures and mineralogy present in the reef package. A chlorine-rich volatile fluid enriched in PGE may have evolved during crystallization of intercumulus liquid below, migrated up through the cumulate pile, and may have redissolved in a vapor-undersaturated intercumulus melt to cause partial melting of the cumulates. This horizon, within which the fluid is redissolved, marks a chemical or physical discontinuity in the pile. Evidence supporting the presence of a chlorine-rich volatile fluid includes the presence of chlorine-rich hydrous phases, pegmatoidal textures, resorbed plagioclase, and hydrous and anhydrous mineral inclusions in chromite and apatite (Boudreau, 1988). Other indications of in-situ formation of the reef are the presence of anorthosites separating the olivine-bearing units from norites and gabbro-norites. These anorthosite layers, with rather sharp contacts, are monomineralic and may represent metasomatic zones (Boudreau, 1988).

The association with pegmatoids argues in favor of a deuteritic or hydrothermal origin for the platinum mineralization. However, the fact that the PGE reef in most of these intrusions is laterally continuous and lies stratigraphically in a similar position with respect to the first appearance of cumulus plagioclase and the reappearance of olivine, is difficult to account for by a hydrothermal process alone. However, this theory could be applied to the Coors anomaly.

## **PHYSICAL DISTURBANCES**

The Lower Banded Series of the Stillwater Complex shows many unusual features which are caused by physical disturbances at the time of formation. Since the Stillwater Complex is a sequence of layered cumulates, magmatic conditions are analogous in this respect to sedimentary environments. Slumping, scouring, cross-bedding, and other sedimentary structures are documented throughout the complex (Foose, 1985). Many of the irregular anomalous features described above for the Coors 602 can be explained by sedimentary processes.

### **Strong Currents, Turbulent Mixing Of Magma, And Magmatic Erosion**

Both the JM and Merensky reef packages show ultramafic xenoliths, slump structures, and disturbed layering suggesting turbulence during mixing (Naldrett et al., 1990). Pulses of magma likely entered the magma chamber numerous times during



formation of the layered complex. Many workers use this idea to explain reversals in fractionation trends upsection in the Stillwater Complex. Turbulent mixing is also needed in models of the JM Reef formation (Campbell et al, 1983; Naldrett et al, 1990). Bow et al. (1982) argue that the ellipsoidal bronzitites directly beneath the JM Reef in the Stillwater Mine area, are xenoliths from the Ultramafic Series. They suggest that the xenoliths are similar to rip-up clasts acquired during times of turbulent mixing. Strong currents could produce scouring in the cumulate pile into which they intrude. The layers through which the JM Reef downcuts in the Coors 602, could have been scoured by strong currents prior to or during Reef formation. The Reef would then form in the trough created .

Bow (1982), Irvine et al. (1983) and Turner et al. (1985), argue that the downcutting features described in the Stillwater mine may represent a pothole. Potholes are believed to be formed from scouring or thermal erosion from a new pulse of magma (Bow, 1982). Buntin et al. (1985) argue that the potholes are scars of the sit of C-H-O-S rich fluids in the new magma are being injected.

Layers in potholes can dip smoothly or drop abruptly into the pothole, or even terminate against the pothole margin. PGE mineralization occurs in the bottom of the potholes, presumably because the reef dips into them. Layers in the Coors area also dip and terminate and mineralization takes an unusual dip in the stratigraphic section (Fig. 5a). Stratigraphic units are missing or thinned due to erosion in forming potholes. This could explain the virtual absence of Gabbronorite I in the Coors 602 area. The reef dips in these

areas and crosscuts stratigraphy along the upper edges of the potholes. Many contacts in the Coors area show the units truncating norite layers, and could mark the upper edge of a pothole (Fig. 17). Faulting and lack of exposure may obscure such an occurrence in the Coors area.

Buntin et al. (1985) describe discordant, pegmatoidal gabbroic dikes, within the potholes, that pinch out a few meters above and below the layers they cut. Some of these rare dikes contain fragments of the pothole margin. Based on these dikes, they proposed a plutonic fumarole model. The bronzitite body along the Fishscale fault, as well as the pods at the base of the Coors-602 area, could be similar to these dikes, in that it crosscuts layering and pinches out in both directions.

One inconsistency in the idea of the Coors area representing one of these potholes is the presence of the JM reef above the lower, anomalous, Coors mineralization. However, without three-dimensional control, the presence of potholes cannot be ruled out. A pothole in the Coors area could extend approximately perpendicular to the strike of the layers and into the rocks, and could have an irregular shape.

### **Topography In The Magma Chamber**

The absence or thinning of units in the Coors area, as mentioned above, could form in other ways besides potholes. Turner et al. (1985), Raedeke and McCallum (1985), and Naldrett (1990) describe variations in thickness in the Ultramafic Zone (Figs. 18 & 19). The Peridotite Zone at Chrome Mountain is about half as thick as that at

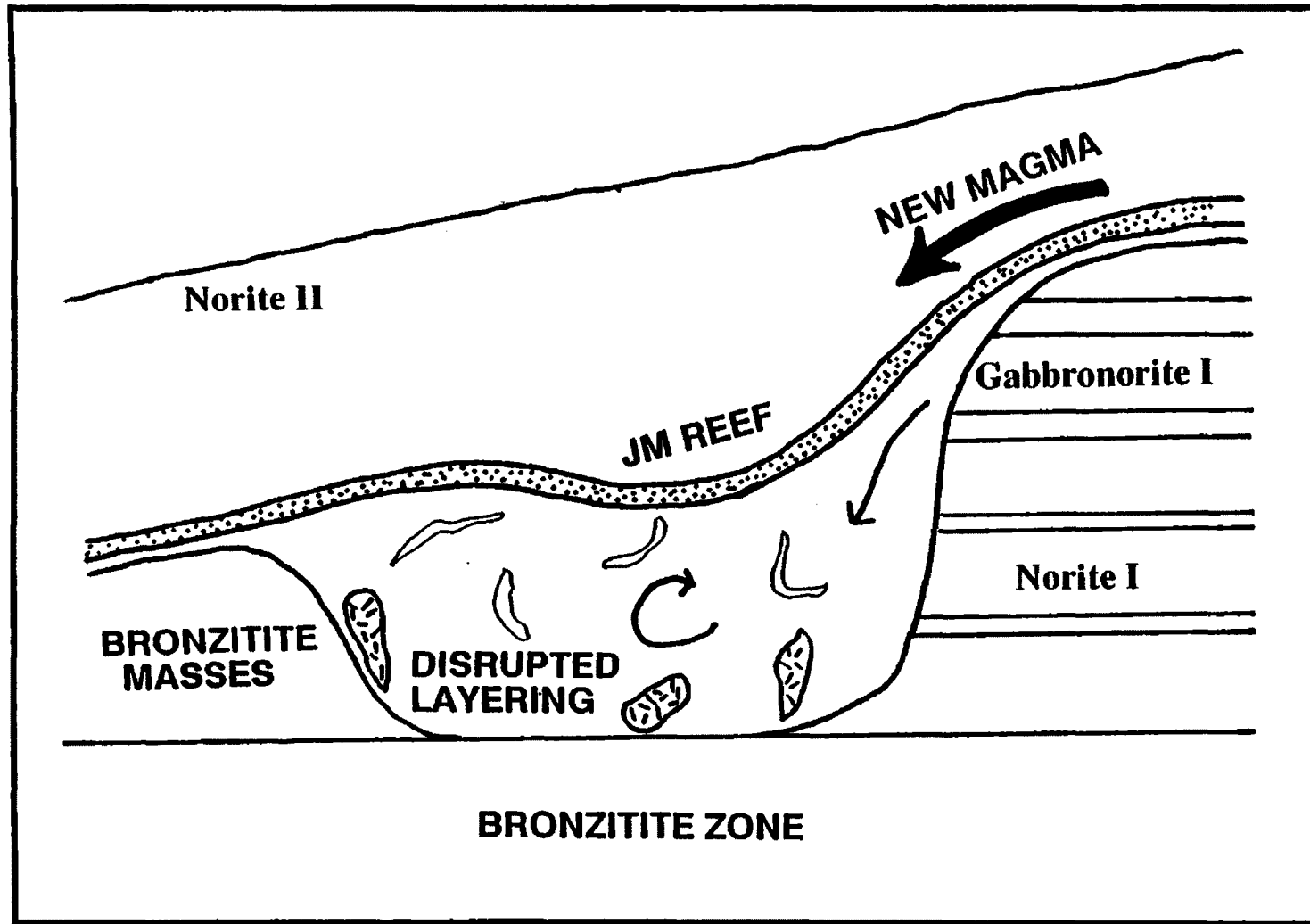


Figure 17. Schematic model of disturbed layering in Coors area caused by an influx of new magma. JM Reef shown in present position after influx of new magma.

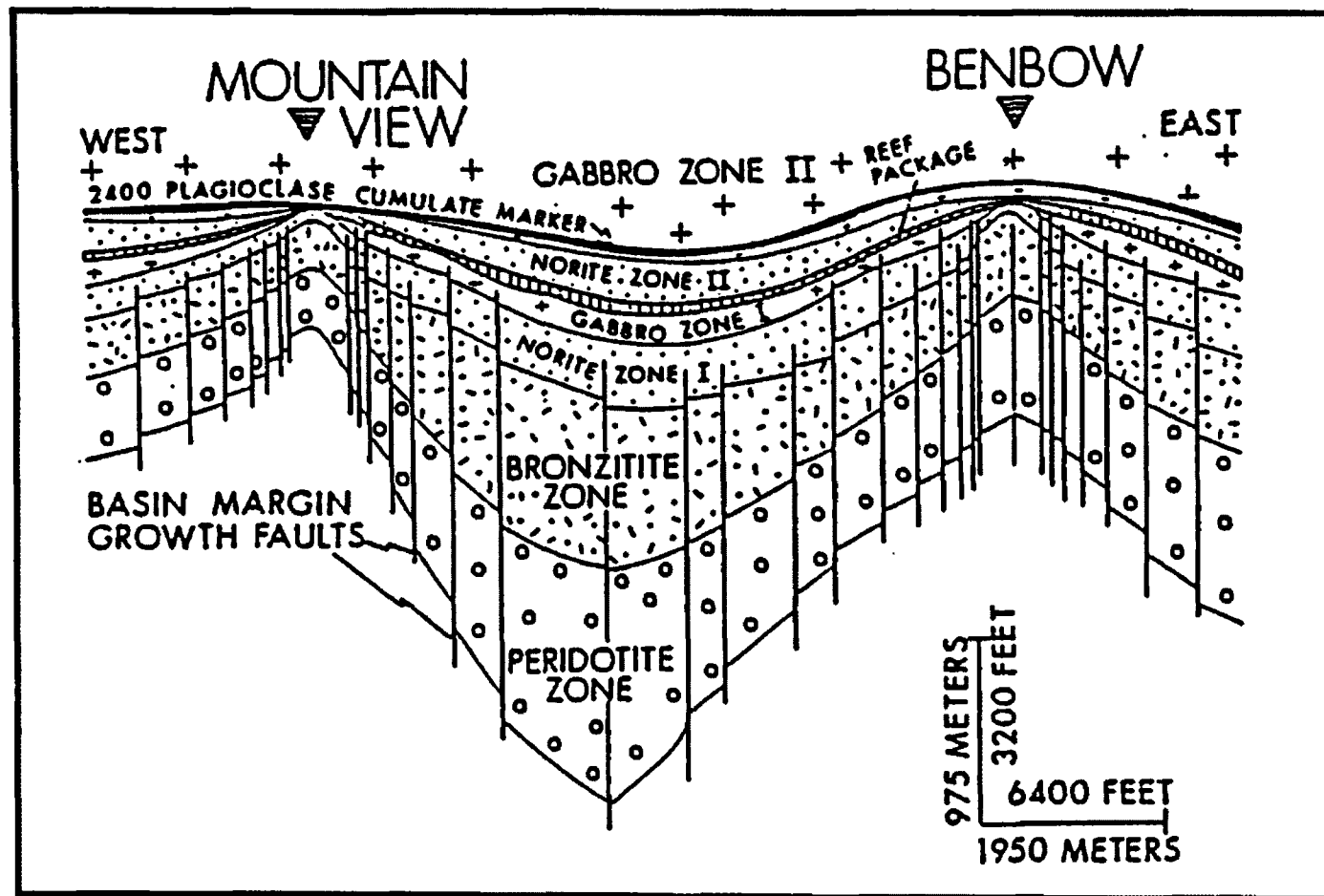


Figure 18. Reconstruction of the base of the Stillwater Complex showing idealized basins and topographic highs at the time of JM Reef deposition (Turner, et al., 1985)

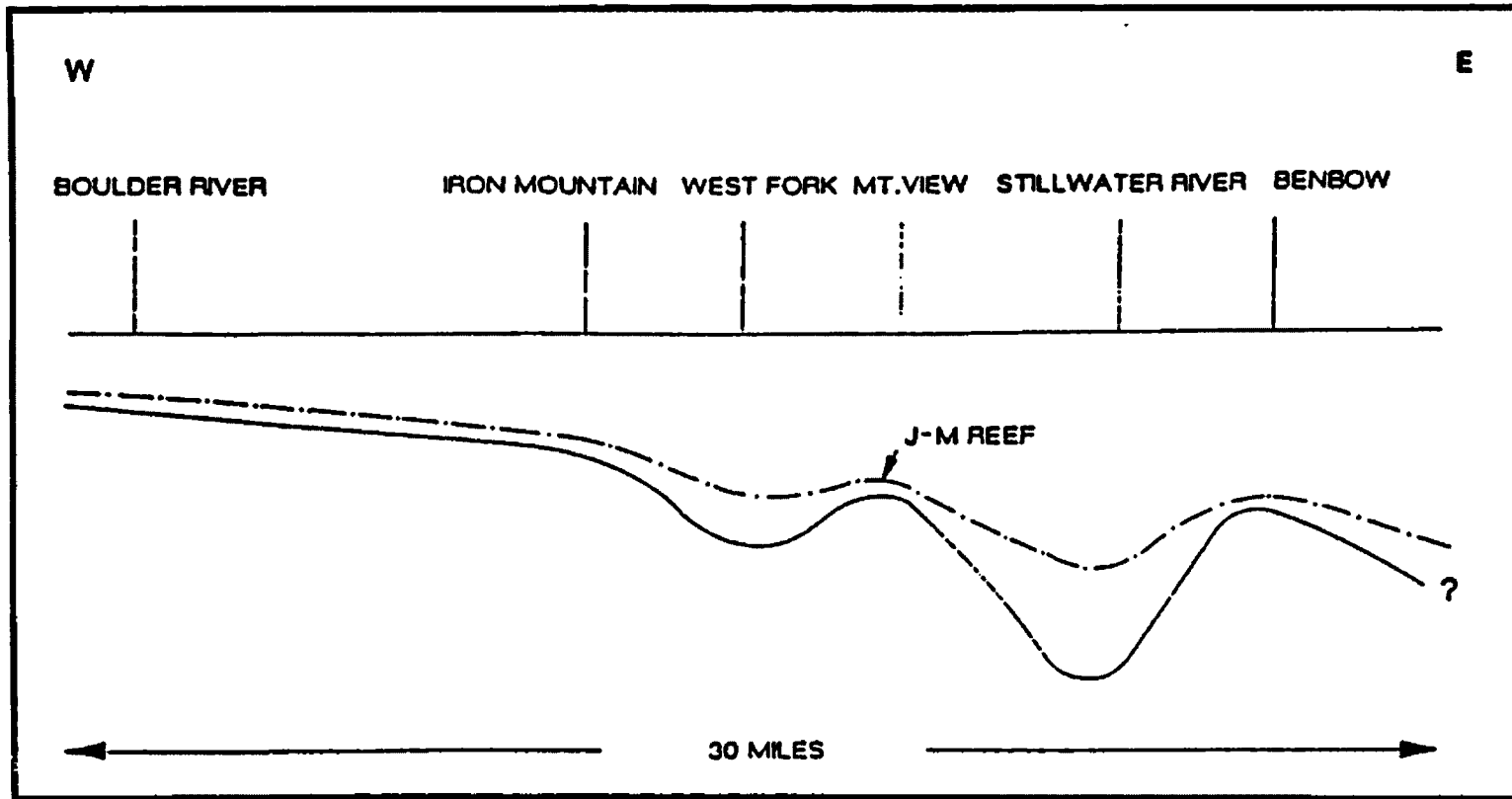


Figure 19. Conceptual view of basin and ridge development before Laramide deformation in the eastern part of the Stillwater Complex (from Turner et al., 1985)

Mountain View (Raedeke and McCallum, 1985). These authors explain the differences as platform versus basinal features formed from magma crystallizing dense, ultramafic cumulates causing the floor of the magma chamber to subside. The thicker Mountain View section forms in the basin, and the Chrome Mountain section forms on a stable platform (Raedeke and McCallum, 1984).

### **Slumping, Compaction, And Faulting During Formation**

Based on field observations and drill core examination, models other than faulting must be used to explain the irregular contacts in the Coors area. Various magmatic processes seem most plausible. A crystals and melt combination creates a layered crystalline mush, which eventually crystallizes to produce the sedimentary-style layering. Crystals forming on a slope, along the crystallizing front or on a topographic high in the chamber, could slump causing compaction (Fig. 20). A load of crystals settled on top of the crystalline mush could also cause compaction in the layers below.

The bronzite masses in the Coors area can also be attributed to sedimentary processes during formation. A disturbance such as compaction, faulting, or slumping during crystallization could not only bring xenoliths up from below, but could also force a bronzite crystal mush up through fractures in the manner of a clastic dike.

The origin of the pegmatoids in the Coors area could possibly be related to the same processes that disrupted the stratigraphy below the reef. Any late-stage movement within the solidifying pile of cumulates could have created channelways to facilitate

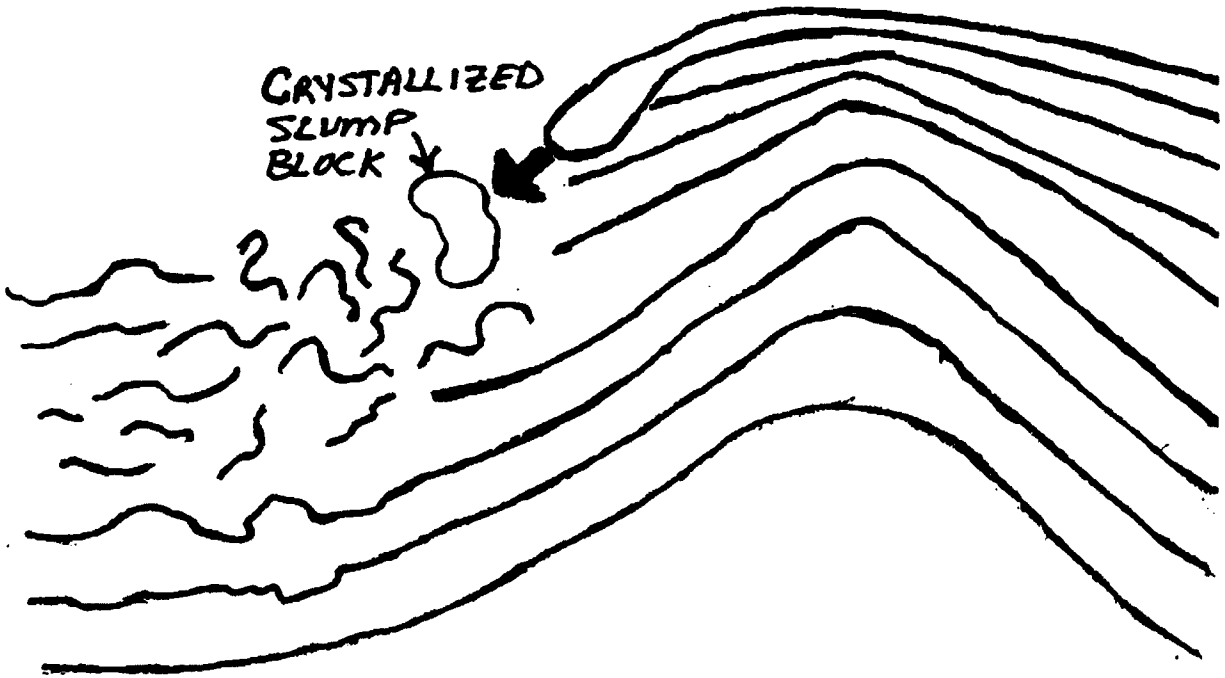


**Figure 20. Schematic diagram showing layering disrupted by a crystallized block slumping off a topographic high in the magma chamber.**

streaming of volatiles separated during late-stage, differentiation. Concentration of volatiles could have inhibited nucleation of late-stage phases thereby forming pegmatoids.

## **CHEMICAL DISTURBANCES**

Not all of the anomalous features in the Coors-602 area can be explained strictly by physical events. Some chemical disturbances are present which may or may not be related to the physical disruptions discussed above.

### **Mg Number**

Naldrett et al. (1987) and Raedeke et al. (1985) give representative Mg numbers for the Stillwater complex. As stated earlier, McCallum suggests an increase in Fe in the Chrome Mountain area (McCallum, 1980). The Mg/(Mg+Fe) content of bronzites of the Bronzite Zone from the Coors and Lost Mountain areas, both relatively close to Chrome Mountain, average 0.83. Although the data from Coors and Lost Mountain may support the suggested increase in Fe in the Chrome Mountain area, the difference in the data does not seem statistically significant enough to use as evidence for Fe increase. However, the bronzite analyses from the Lower Banded Zone do show a significant Fe increase.

The Mg/(Mg+Fe) values of samples from the Coors area show some interesting relationships. An upward decrease, as seen in groups A and E in Figure 10, in Mg numbers in bronzites is what one would expect through differentiation. Bronzites from the unmineralized samples have a slightly higher Mg number. Mineralized samples from



the lower Banded Series and along the bC “dike” have low Mg numbers as compared with reef samples (group D1) which have high magnesium numbers. If mineralization of PGE-bearing sulfides caused the iron increase in the bronzitite samples from the Banded-Ultramafic contact, one would expect PGE-bearing sulfides to cause a similar iron increase in reef samples. The reef samples do not show an iron increase and they are not far off the fractionation trend (groups E and C in Fig. 10). These results are evidence that the iron increase in the anomalous bronzitites in the Norite I Zone is due to some other event, not the presence of sulfides.

One explanation for the presence of bronzitites in the lower Banded Series is the possibility that they are xenoliths from the Bronzitite Zone. Assuming the bronzitite masses in the Norite I Zone of the Coors-602 area are xenoliths detached from the Bronzitite Zone, the chemical signatures should be similar and an upward decrease in Mg number should not occur. In Coors, the Mg numbers of orthopyroxenes from unmineralized bronzitites in the lower Banded Series is similar to Mg numbers of samples analyzed from the Bronzitite Zone. These unmineralized samples may represent xenoliths from the Bronzitite zone. The mineralized bronzitites, however, have low Mg numbers. The possibility that these mineralized bronzitites are xenoliths from the Bronzitite Zone can therefore be ruled out.

## **Resorption**

An injection of a new batch of magma, as proposed for the formation of potholes (Bow et al., 1982; Buntin et al., 1985; Vermaak and Von Gruenewalt, 1981), as well as the formation of the reef (Naldrett et al., 1990; McCallum et al., 1980, and others) and cyclic units, is consistent with the textures observed in the Coors samples. Many of the bronzites exhibit a resorbed or remelting texture. The grains not only have rounded boundaries, but they contain numerous embayments as if they have come in contact with a melt with which they were not in equilibrium. If the intercumulus melt around the bronzites mixed with a more fractionated melt from above, the bronzite would become unstable. Volatile influx could also cause instability of bronzite grains.

## **Increase in $f_{H_2O}$**

Raedeke and McCallum (1984), suggest an increased water fugacity during crystallization in the Chrome Mountain vicinity could cause an increase in Fe in orthopyroxene relative to those from Mountain View. The presence of numerous pegmatoids, some of which contain phlogopite, along the Ultramafic-Banded Series contact in the Coors area, and the presence of secondary dunite lower in the section, support the idea of increased  $f_{H_2O}$ . Stumpfl and Rucklidge (1982) suggest that Fe-rich hydrous fluids rising through the cumulate pile form similar dunite pipes in the Bushveld Complex by a metasomatic origin. Pegmatoidal pyroxenite near the pipes in the Bushveld

shows an increase in Fe content compared to nearby pyroxenites (Stumpfl and Rucklidge, 1982). Schiffries (1982) suggests that the plagioclase in the dunites was removed by hydrolysis and olivine was produced by removal of silica from pyroxene. He argues that the pipes represent conduits for intercumulus flow of Fe-rich hydrous fluid.

Assuming the discordant dunites in the Stillwater formed the same way as those in the Bushveld, the Fe-rich hydrous fluid responsible for the formation of dunite could have migrated upwards through fractures, equilibrating with interstitial melt, thereby becoming silica saturated. Instead of Fe-rich, Si-undersaturated hydrous fluids, the hydrous fluid, once in the Banded Series, was probably Fe-rich and Si-saturated, thus forming bronzitites rather than dunites. The infiltrating fluids also would have provided the necessary mixing needed for PGE to collect in the sulfides (Naldrett et al, 1990). The disrupted stratigraphy in the Coors area could have been caused by volume change due to dissolution of plagioclase (Schiffries, 1982).

Schiffries (1982) suggests that the location of the pipes is structurally controlled, the metasomatizing fluids flowing through irregular channelways along structural weaknesses. Naldrett et al. (1987) mention the possibility of growth faults forming along the margins of basins in the magma chamber. Such faults could have been the structural weaknesses in which these pipes formed. He suggests pegmatoids could have formed as open-space filling when fluids crossed over fractures and crystallized rapidly. The large Fishscale fault zone in which some of bronzitite occurs could be a reactivated growth fault.

### **PGE Mineralization Below the JM Reef**

Irvine et al. (1983) argues that a dissolved volatile component, especially water, diffuses faster than other components and could be the dominant component in mixing by double-diffusive convection. If this is the case, and water is present in the melt, mixing could be triggered earlier or more extensively than in areas with less water. Evidence is presented above for elevated amounts of water in the Coors area; thus the onset of mixing could have been earlier, that is lower in the stratigraphic section. If mixing did not begin until the Olivine-bearing Zone I had formed, as elsewhere in the Stillwater, the presence of water could have brought the mixing horizon down to the present position in the Norite I Zone seen in the Coors-602 area.

Naldrett et al. (1990) show that the R factor, the ratio of silicate to sulfide in the melt, must be sufficiently high for PGE sulfides to form. Mixing with large volumes of new magma would have accomplished this to form the JM reef. Considering the Coors mineralization, mixing must have occurred in the lower Norite I Zone prior to deposition of the JM reef. Alternatively, some of the hybrid melt from the mixing horizon, where the reef subsequently formed, could have migrated to the Coors area and deposited the PGE sulfides.

The fact that the Pd/Pt values are lower in the Coors-602 area than in the reef, and that the overall PGE content of the Coors 602 zone is less than the Reef, and that the mineralized bronzitites have higher Mg numbers than mineralized reef rock may suggest that the Coors mineralization had a different origin from the reef.

## **SUMMARY AND CONCLUSION**

The Coors-602 area contains numerous irregular features including disturbed stratigraphy, PGE mineralization below the reef, absence of the Gabbro-norite I, discordant pegmatoidal bronzitites, and low Pd/Pt ratios. Because the sulfides in the Coors area contain significant PGE values, although presently uneconomic, it is important to determine whether the area is just a random anomaly, or this stratigraphic location represent another possible ore horizon. The irregular features in the Coors area are likely genetically associated with the PGE-bearing sulfides. A viable model needs to encompass all such features. Two models, based on data from this work, are proposed below.

### **Model 1**

The Coors-602 area is the first recognized outcrop exposure of a pothole in the Stillwater Complex. Because the region was on a topographic high in the magma chamber and in an overall thinner portion of the complex, crystallization occurred slightly earlier than other areas. Crystallized blocks slumped to cause disruption of the layers below. Bronzite masses from the Ultramafic Series were ripped up during this process. An influx of a new magma caused further disruption in the layers. Layering disturbed just prior to Reef deposition, provided the necessary surface irregularity needed for the onset of pothole formation. Scouring or thermal erosion caused the downcutting to form the pothole. When the new magma came in contact with the bronzite masses, the bronzites became unstable and resorbed. Volatiles fostered formation of pegmatoids in the

bronzitites as well as the reef. The  $f_{H_2O}$  of the volatiles thus increased the iron content in the bronzitites. When the layering was disrupted, conduits were created through which mixed magma (high R value), which ultimately formed the JM reef, flowed down into bronzitite masses precipitating PGE-bearing sulfides. The highly mixed magma, which later precipitated the sulfides with the greater amounts of PGE in the reef, did not mix with the bronzitites below.

## **Model 2**

Syndeponstional “growth” faulting occurred during formation of the Stillwater complex. These faults created conduits through which Cl-rich volatiles, produced by metamorphosing the country rocks below, could flow. The location of the dunite “pipes”, at Chrome Mountain represents one such fault. Volatiles rose through this fault, caused recrystallization of bronzitites in the Peridotite Zone to form the dunite “pipes” and continued up to the Coors area. These volatiles created pegmatoids, resorbed bronzites, and increased the  $f_{H_2O}$  which increased the iron content in upper Bronzitite Zone. The Cl- rich volatiles scavenged PGE along the way upsection. The PGE’ mixed with the sulfide-saturated bronzites, and occasionally norites, to form the anomalous mineralization in the Coors area. The PGE in the volatiles had a low Pd/Pt ratio. A new magma injection, just above the Coor level, along with continued movement along the syndepostional fault, disrupted the stratigraphy in the Coors area. The disturbed layering provided the

necessary surface irregularity needed for the onset of pothole formation. Scouring or thermal erosion caused downcutting to form the pothole in which the JM reef formed.

Both of these models account for the disrupted stratigraphy, the pegmatoidal bronzitites, the PGE-bearing sulfides, and the absence of Gabbronorite I in the Coors 602 zone. Some combination of these two models may represent the best viable genetic process to explain this anomalous zone. In both models, the possibility exists that enough PGE could concentrate to form an economic ore zone. The concentrating process did not go far enough in the Coors area to make it economic. The process did, however, go far enough to provide insight as to how such an anomaly could form and where one would look for other anomalies of this sort elsewhere in the Stillwater and other layered mafic intrusions.

**REFERENCES**

- Boudreau, A.E., and McCallum, I.S., 1992, Concentration of platinum-group elements by magmatic fluids of layered intrusions, *Economic Geology*, v.87, P. 1830-1848.
- Boudreau, A. E., 1988, Investigations of the Stillwater Complex. IV. The Role of Volatiles in the Petrogenesis of the JM Reef, Minneapolis Adit Section: *Canadian Mineralogist*, v. 26, p. 193-208.
- Bow, C., Wolfgram, D., Turner, A., Barnes, S., Evans, J., Zdepski, M., and Boudreau, A., 1982, Investigations of the Howland Reef of the Stillwater Complex, Minneapolis Adit Area: Stratigraphy, Structure, and Mineralization: *Economic Geology*, v. 77, p. 1481-1492.
- Buntin, T.J., Grandstaff, D.E., Ulmer, G.C., and Gold, D. P., 1985, A pilot study of geochemical and redox relationships between potholes and adjacent normal Merensky reef of the Bushveld Complex: *Economic Geology*, v. 80, p. 975-987.
- Browdowski, R.A., Ulmer, G.C., Bonini, W.E., and Gold, D.P., 1982, The Stillwater stratiform complex: New evidence for its northern extent: *Geological Society of America Abstracts with Programs*, v. 14, p.453.
- Campbell, I.H., 1978, Some problems with the cumulus theory: *Lithos*, V. 11, p.311-323.
- Campbell, I. H., Naldrett, A. J., and Barnes, S. J., 1983, A model for the origin of the platinum-rich sulfide horizons in the Bushveld and Stillwater Complexes: *Journal of Petrology*, v. 24, p. 133-165.
- Conn, H.K., 1979, Discovery and evaluation of the Johns-Manville platinum-palladium prospects, Stillwater Complex, Montana, USA: *Canadian Mineralogist*, v. 17, p. 463-469.
- Foose, M.P., 1985, Primary structural and stratigraphic relations in Banded-series cumulates exposed in the East Boulder Plateau-Contact Mountain area, *in* Czamanske, G.K. and Zeintek, M.L., *The Stillwater Complex, Montana Geology and Guide* Montana Bureau Mining and Geology Special Publication, 92, p.305-324.
- Hess, H.H., 1960, Stillwater igneous complex, Montana - a quantitative mineralogical study: *Geological Society of America Memoir* 80, 230p.



- Howland, A.L., 1955, Chromite deposits in the central part of the Stillwater Complex, Sweet Grass County, Montana: U.S. Geological Survey Bulletin 1015-D, p.99-121.
- Hyndman, D.W., 1985, *Petrology of Igneous and Metamorphic Rocks*, McGraw Hill Inc., New York, p.61.
- Irvine, T.N., 1980, Magmatic Density Currents and cumulus processes: *American Journal of Science*, vol.280-A, part 1, p.1-58.
- \_\_\_\_\_, 1980, Magmatic infiltration metasomatism, double-diffusive fractional intrusions: *in* Hargraves, R.B.,(ed.), *Physics of Magmatic Processes*, Princeton University Press, New Jersey, p.325-383.
- Irvine, T.N., Todd, S.G., and Keith, D.W., 1983, The J-M platinum-palladium reef of the Stillwater Complex, Montana:II. Origin by double-diffusive convective magma mixing and implications for the Bushveld Complex: *Economic Geology*, v. p.1287-1348.
- Jackson, E. D., 1961, Primary Textures and Mineral Associations in the Ultramafic Zone of the Stillwater Complex, Montana: *Geological Survey Professional Paper* 358, 106 p.
- Jones, W.R., Peoples, J.W., and Howland, A.L., 1960, Igneous and tectonic structures of the Stillwater Complex, Montana: *Geological Survey Bulletin* 1071-H, P.281-340.
- Kinloch, E., and Peyerl, W., 1986, The Union Section of Rustenburg Platinum Mines Limited with reference to the Merensky Reef: *in* Mineral Deposits of Southern Africa, Anhaeusser, C. R. and Maske, S. (eds), Vol. I and II, Geological Society of South Africa, Johannesburg, p. 1061-1090.
- Kleinkopf, M.D., 1985, Regional gravity and magnetic anomalies of the Stillwater Complex area: *in* Czamanske, G.K. and Zeintek, M.L., *The Stillwater Complex, Montana Geology and Guide* Montana Bureau Mining and Geology Special Publication, 92, p.33-38.
- Lambert, D.D., 1982, Geochemical evolution of the Stillwater Complex, Montana: Evidence for the formation of platinum-group element deposits in mafic layered intrusions [Ph.D thesis]: Colorado School of Mines, Golden, Colorado, 274 p.
- Lipin, B.R., 1993, Pressure increases the formation of chromite seams and the developments of the ultramafic series in the Stillwater Complex, Montana: *Journal of Petrology*, V. 34, no.5, p.955-976.

- Mathez, E. A., Dietrich, V. J., Holloway, J. R., and Boudreau, A. E., 1989, Carbon distribution in the Stillwater Complex and evolution of vapor during crystallation of Stillwater and Bushveld magmas: *Journal of Petrology*, v. 30, p. 153-173.
- McCallum, I.S., Raedeke, L. D., and Mathez, E.A., 1980, Investigations of the Stillwater Complex: Part I. stratigraphy and structure of the banded zone: *American Journal of Science*, vol. 280-A, part 1, p.59-87.
- McCallum, I.S., Raedeke, L.D., Mathez, E.A., and Criscenti, L.J., A traverse through the Banded series in the Contact Mountain area: *in* Czamanske, G.K. and Zeintek, M.L., *The Stillwater Complex, Montana, Geology and Guide* Montana Bureau Mining and Geology Special Publication, 92, p. 293-304.
- Naldrett, A.J., Cameron G., von Gruenewaldt G., and Sharpe M.R., 1987, The formation of stratiform PGE deposits in layered intrusions, *in* *Origins of Igneous Layering*, Parsons, I. (ed): D.Reidel Publishing Company, p.313-397.
- Naldrett, A. J., Brugmann, G. E., and Wilson, A. H., 1990, Models for the concentration of PGE in layered intrusions: *Canadian Mineralogist*, v. 28, p. 389-408.
- Page, N. J, Stillwater Complex, Montana; Rock succession, metamorphism and structure of the complex and adjacent rocks: U.S. Geological Survey Professional Paper 999, 79 p.
- Page, N. J., and Moring, B.C., 1990, Petrology of the noritic and gabbro-noritic rocks below the J-M reef in the mountain view area, Stillwater Complex, Montana: U.S. Geological Survey Bulletin 1674-C, 47p.
- Page, N.J., and Nokleberg, W.J., 1974, Geologic map of the Stillwater Complex, Montana: U.S. Geological Survey Miscellaneous Investigation Series I-797.
- Page, N.J., and Zientek, M.L., 1985, Geologic and structural setting of the Stillwater Complex: *in* Czamanske, G.K. and Zeintek, M.L., *The Stillwater Complex, Montana, Geology and Guide* Montana Bureau Mining and Geology Special Publication, 92, p.1-8.
- Page, N.J., Zientek, M.L., Czamanske, G.K, and Foose, M.P., 1985, Sulfide mineralization in the Stillwater Complex and underlying rocks: *in* Czamanske, G.K. and Zientek, M.L., *The Stillwater Complex, Montana, Geology and Guide* Montana Bureau Mining and Geology Special Publication, 92, p. 93-96.
- Raedeke, L.D., 1986, A three dimensional view of mineralization in the Stillwater J-M reef: *Economic Geology*, vol. 81, part 5, p. 1187-1195.

- Raedeke, L.D. and McCallum, I.S., 1982, Modal and chemical variations in the Ultramafic zone of the Stillwater Complex, *in* Workshop on magmatic processes of early planetary crusts: Magma oceans and stratiform layered intrusions, Walker, D., and McCallum, I.S., (eds.): Lunar and Planetary Institute, Houston, Texas, LPI Technical Report 82-01, p. 135-137.
- \_\_\_\_\_ 1984, Investigations in the Stillwater Complex: part II. Petrology and petrogenesis of the Ultramafic Series: *Journal of Petrology*, v. 25, p. 395-420.
- \_\_\_\_\_ 1985, A guide to the Chrome Mountain area, *in* Czamanske, G.K. and Zientek, M.L., *The Stillwater Complex, Montana, Geology and Guide* Montana Bureau Mining and Geology Special Publication, 92, p. 277-285.
- Raedeke, L.D., McCallum, I.S., Mathex, E.A., and Criscenti, L.J., 1985, The Contact Mountain section of the Stillwater Complex, *in* Czamanske, G.K. and Zientek, M.L., *The Stillwater Complex, Montana, Geology and Guide* Montana Bureau Mining and Geology Special Publication, 92, p. 286-292.
- Schiffries, C. M., 1982, The petrogenesis of a platiniferous dunite pipes in the Bushveld Complex: Infiltration metasomatism by a chloride solution: *Economic Geology*, v. 77, p. 1439-1453.
- Seegerstrom, K., and Carlson, R.R., 1982, Geologic map of the banded upper zone of the Stillwater Complex and adjacent rocks, Stillwater, Sweet Grass, and Park Counties, Montana: U.S. Geological Survey Map I-1383.
- Spry, A., 1979, *Metamorphic Textures*, Pergamon Press, Oxford.
- Stumpfl, E. F., and Rucklidge, J. C., 1982, The platiniferous dunite pipes of the Eastern Bushveld: *Economic Geology* v. 77, p. 1419-1431.
- Todd, S.G., Keith, D.W., Leroy, L.W., Schissel, D.J., Mann, E.L., and Irvine, T.N., 1982, The J-M platinum-palladium reef of the Stillwater Complex, Montana: I. Stratigraphy and petrology: *Economic Geology*. vol. 77, p. 1454-80.
- Turner, A.R., Wolfram, D., and Barnes, S.J., 1985, Geology of the Stillwater County sector of the J-M reef, including the Minneapolis adit: *in* Czamanske, G.K. and Zientek, M.L., *The Stillwater Complex, Montana, Geology and Guide*, Montana Bureau Mining and Geology Special Publication, 92, p. 210-230.
- Vermaak, C. F., 1976, The nickel pipes of Vlakfontein and vicinity, Western Transvaal: *Economic Geology*, v. 71, p. 261-286.

- Vermaak, C.F., and von Gruenewaldt, G., 1981, Third International Platinum Symposium: Johannesburg, Geological Society of South Africa, 62 p.
- Viljoen, M. J. and Hieber, R., 1986, The Rustenburg Section of Rustenburg Platinum Mines Limited, with reference to the Merensky Reef: *in* Mineral Deposits of Southern Africa, Anhaeusser, C. R., and Maske, S.(eds.), Vols I and II, Geological Society of South Africa, Johannesburg, p.1107-1134.
- Viljoen, M. J., and Scoon, R. N., 1985, The distribution and main geologic features of discordant bodies of iron-rich ultramafic pegmatite in the Bushveld Complex: *Economic Geology*, v. 80, p.1109-1128.
- Volborth, A., 1985, Sulfide and associated platinoid mineralization in the Stillwater "reef" and underlying graphite-pyroxenite pegmatoids: Montana Bureau of Mines and Geology Open File Report No. 161, 105 pp.
- Volborth, A., and Housley, R.M., 1984, A preliminary description of complex graphite, sulphide, arsenide, and platinum group element mineralization in a pegmatoid pyroxenite of the Stillwater Complex, Montana, U.S.A.: *TMPM Tschermaks Mineralogische und Petrographische Mitteilungen*, v.33, p.213-230.
- Zientek, M.L., Czamanske, G.K., and Irvine, T.N., 1985, Stratigraphy and nomenclature for the Stillwater Complex: *in* Czamanske, G.K. and Zientek, M.L., *The Stillwater Complex, Montana, Geology and Guide* Montana Bureau Mining and Geology Special Publication, 92, p. 21-32.

## APPENDICES

**Appendix A: Outcrop map (1" =100') prepared by geologists at the Stillwater Mining Co. and Johns-Manville (in pocket)**

**Appendix B: USGS Geochemical Analyses  
(3.5 floppy disk - IBM format) (in pocket)**